Umm Al-Qura University Journal of Engineering & Architecture

Volume 4 Number 2 Rajab 1433, June 2012

Registered at
Umm Al-Qura University
Under Legal Deposit No. 247/1433-2012/ISSN 1658-4635

Printed in the Kingdom of Saudi Arabia by
Umm Al-Qura University Press
http://www.uqu.edu.sa
email: jea@uqu.edu.sa

ISSN 1658-4635

مطابع جامعة أم القرى

Registered at
Umm Al-Qura University
Under Legal Deposit No. 3168/20/1432-2012/ISSN 1658-4635

Printed in the Kingdom of Saudi Arabia by
Umm Al-Qura University Press
http://www.uqu.edu.sa
email: jea@uqu.edu.sa

Umm Al-Qura Univ. J. Eng.& Arch.

Aims and Scope

The Journal publishes original research, reviews and cases reports in the Arabic and English languages in the fields of Engineering and Architecture. Manuscripts will be reviewed by the editors and the appropriate referees.

Visit University Web Site
http://www.uqu.edu.sa
email: jea@uqu.edu.sa

3168/20/1433-2012 © The University Press

Instructions to Authors

Umm Al-Qura University Journal for Engineering and architecture is please to published original research, scientific revision and reports.
The submitted manuscript should be on white paper size A4, original and four copies (photographs should be five original). Should be typed double-space with a 3 cm margin in all sides, Using time roman font size 12 normal for the text, use size 12 bold upper case for main title. Submitting must be directed to Editor-in-chief with a letter of submission stating that the manuscript sent to this journal has not been submitted or published elsewhere. In case of co-authors a letter of delegation to corresponded author should be attached. The content of the manuscript should follow the following order.

1- Title page with author's name, affiliation and address.

2- Title Page (Page numbering starts from this page).

3- Summary followed by a list of key words (should not exceed 10 words).

4- Text should follow the following order: Introduction, Methods, Results, Discussion, Acknowledgments, References, Tables, Figures, and Photographs. And legend of tables, figures, and photographs if necessary.

Title should not exceed 20 words and should represent the content of the manuscripts, or indicate main finding (conclusion), (use size 16, Bold).

Authors Names should be in English and Arabic in the following order:
First Name --- Middle name --- Surname OR initials followed by surname accompanied with affiliations and full address of the author. (use size 12, Bold)

Summary should be in English and Arabic (Approx. 250-300 words) and should indicate the aim, execution of the work and the findings.

Introduction should include the purpose and justification of the project. Primary references should not exceed 15. Should not include methods, data, results, discussion, or conclusion from the work being reported.

Materials and Methods should be precise, clear, complete and objectively acceptable to the readers.

Results should be presented in a clear and logical sequence in the text avoiding repetition of data given in Tables and figures. Results should be supported by appropriate statistics.

Discussion should be pertinent to the data presented, findings and conclusions. It should be clearly related the objective of the study with a reference to previous relevant studies.

Acknowledgements should be as brief as possible.

References should be pouted in the text with authors name and date of publication in parenthesis, and listed at the end of the paper in alphabetical order.*

Tables should be typed on a separate sheet using double spacing. The size of the of the table should not exceed 13 18cm. Table number and informative heading should be written at the top of table. Table number and heading with footnotes legends (abbreviations, comments, and statistical treatment) should be provided on another separate sheet.

Figures and photographs should be provided on a separate sheet size 10x12cm. Legends should enable the reader to understand the information contained in figures, or tables without reference to the text.

Units The recommended System International (SI) units should be used.

Offprint Author will receive fifteen off-prints free of charge. Extra copies can be ordered when the proofs are returned. Price will be indicated on the order form.

***References** are indicated in the text by Harvard System (name and date). e.g "Recent studies (Sultan 1996; Al-Amoudi 1997; Richards 1998) found....." or Recently, Sultan (1998) found.....". When referring to a work by more than two authors, give the name of the first author followed by et al. (Fjuimoto et al. 19992). More than one work by the same author(s) in the same year should by the letters a, b etc. Following the year of publication. The name of the journal should be written as in the Index Medicus. For example:

Journal Paper

Chen, L. & Twu, H.1995. Synthesis of multilevel NAND gati circuits for incompletely specified multi-output Boolean functions and **CAD** using permissible cubes and **PCRM** graphs. International Journal of Electronics 78 (2): 303-319.

Reusch, B. 1975. Generation of prime implicants from sub functions and a unifying approach to the covering problem. *IEEE* Transactions on Computers C-24: 924 – 930.

Bartee, T.C.1969. Computer design of multiple output logical networks. *IEEE* Transactions on Electronic Computers EC-10 (1): 21-30.

Book

Jenny, H. 1980. The soil resource. Springer-Verlag, Berlin, 377pp.

Muroga, S. 1974. Logic design and switching theory. Wiely, New York, 617 pp.

Edited volume or Book chapter

Kaszab, Z. 1981. Coleoptera: Family Tenebrionidae. In: Fauna of Saudi Arabia (Edited by Wittmer, W.&Buttiker, W.) Vol. 1, pp257-288. Ciba-Geigy, Basel, Switzerland.

Conference or Symposium Paper

Darwish, M.A. 1983. Better arrangement of desalting plants using multi effect boiling system. The |First Saudi Engineering Conference, King Abdul Aziz University, Jeddah, Saudi Arabia.

Dissertation.

Yilbas, B.S. 1985. Heat transfer mechanisms initiating the laser drilling of metals. Ph.D. thesis, University of Birmingham, U.K.

3168/20/1433-2012 © The University Press

To Home It May Concern

Author Name:

Scientific Position:

Department:

College:

University:

Paper Title:

Co-author (if any):

I herby sign on the behave of myself (and co-author's, if any) that this paper has not published nor send for publication to any other journal locally or internationally. And I am welling to follow authors instructions at Umm Al-Qura University Journal of Engineering & Architecture.

Author Signature Date:

3168/20/1433-2012

DATABASE

Please fill in following details, in order that we can update our database.

TITLE: .....

SURNAME:.....

FIRST NAME:.....

SPECIALTY:.....

INSTITUTE:.....

ADDRESS:.....

TEL NO. :.....

FAX NO. :.....

E-MAIL:.....

Volume 4 Number 2 –Rajab 1433 June 2012

ARABIC SECTION

This Volume does not include Papers in Arabic

Mechanics

Umm Al-Qura Univ. J. Eng.& Arch. Vol. 4, No.2, pp. 37-53 (2011) 32-9-012 © The University Press 15-26

Three-Dimensional Finite Element Analysis on Thermal Stress in a Brake Drum of Heavy Commercial Truck

Khairul Fuad[1], Mohammed Wasel Al-Hazmi[1], Awaluddin Th.[2], and Th. Hemchi[3]

1) Dept.of Mech.Engineering, Umm Al-Qura University, Kingdom of Saudi Arabia
2) Dept.of Mech.Engineering, University of Sumatera Utara, Indonesia
3) Dept.of Mech.Engineering, PETRONAS University of Technology, Malaysia.
E-mail: khairulfuad@petronas.com.my

تحليل الإجهادات الحرارية لأسطوانة الفرامل للشاحنات التجارية باستخدام نظرية العناصر المحدودة

الملخص

يولد استخدام الفرامل في الشاحنة التجارية الثقيلة عند السرعات العالية حرارة مفرطة على السطح عند الاحتكاك مع اسطوانة الفرامل. قد تسبب هذه الحالة آثار غير مرغوب فيها على اسطوانة الفرامل التي تؤدي في نهاية المطاف إلى بداية ظهور في الشقوق الحرارية. ومن أجل تصميم أمثل لأسطوانة الفرامل تكمن أهمية فحص الإجهاد الحراري نتيجة لدرجات الحرارة المفرطة الناتجة عن احتكاك سطح الأسطوانة بالفرامل عند الكبح. تقوم هذه الدراسة بتحليل الإجهاد الحراري على اسطوانة الفرامل للشاحنات التجارية الثقيلة باستخدام نظرية العناصر محدودة ثلاثي الأبعاد كمرحلة الأولى وذلك لتحليل الصدع الناتج عن الحرارة المفرطة نتيجة الاحتكاك على اسطوانة الفرامل. تقوم الدراسة على تحليل تأثير اثنين من دواسات الفرامل على اسطوانة الفرامل، ونتيجة التسخين والتبريد الذي يحدث تعاقبياً على اسطوانة الفرامل أثناء استعمال الفرامل. تم تطبيق الدراسة عند على حالة استخدام شدة تأثير الفرامل عند التباطؤ بقيمة تساوي نصف تسارع الجاذبية الأرضية. بينت نتائج الدراسة أن أكبر قيمة مسجلة للحرارة الناتجة عن الاحتكاك عند منتصف المسافة من بداية الكبح. بينما تصل أعلى قيمة للإجهاد الحراري عند ربع وقت حصول الكبح.

Summary

Brake application in a heavy commercial truck running with high speed will generate an excessive thermal environment on the frictional surface of brake drum. This condition may cause undesirable effects on the material of the brake drum that eventually lead to the initiation of heat cracks. Therefore, for optimized design of a brake drum, it appears to be very important to examine the thermal stress due to the excessive temperature in the rubbing surface of the brake drum in the course of braking. This paper reports a 3-D finite element analysis on thermal stress in a brake drum of heavy commercial truck as the first stage of investigating the initiation of heat crack in the brake drum. The braking is done by two brake shoes, and the heating and cooling occur alternatively in the brake drum during the brake application. A severe brake application with deceleration $0.5g$ is taken into account. The history of the transient temperature and thermal stress in the course of braking are plotted and discussed. It is found that the maximum temperature occurs when the braking time is reaching a half-way, whilst the maximum thermal stress occurs when it is reaching at around one-fourth of braking time.

Key-words:

Brake drum, 3-D finite element analysis, transient temperature, thermal stress.

INTRODUCTION

Friction brakes are widely used to provide an inexpensive, consistent and reliable means of retardation, and conveniently, generate large frictional forces to give high rates of deceleration. A severe thermal environment is created at such a friction interface and satisfactory braking performance largely depends on the effective dissipation of heat energy from this interface.

Up to now, the drum cracking of heavy and large commercial vehicle has become a widespread problem caused by thermal damage due to excessively high surface temperature in the course of brake application. The brake drums are prone to overheat on long down-grades because they must be braked more frequently under high speed braking and heavier load.

Nowadays, the predominant trend in the development of large vehicles is toward higher speeds and heavier loads, which increases considerably the energy required to be dissipated by the brake drum, and, consequently, it will generate excessive temperature that produce high thermal stresses. This condition may cause undesirable effects on the material of the brake drum that eventually lead to the initiation of heat cracks.

The investigation of transient temperatures, thermal stresses, and thermal distortions in brake drum have been extensively performed by the brake drum designers and researchers attending to this field. Most thermal analyses assume that the heat generated during braking is uniformly distributed over the nominal area of contact between lining and drum. In practice, manufacturing tolerance and drum distortion give rise to non-uniform contact and the frictional heat is generated over discrete areas forming a band or bands whose total width is less than the total band width of the lining material.

The finite element analysis is a powerful technique for the solution of many engineering problems, and has been extensively used for thermal analysis applied to the brake components. Three-dimensional analysis on temperature distribution in a brake drum using finite element method has been reported by Khairul Fuad et al. 2008. Some other papers analyzing the thermal analyses in brake drum in two dimensional analyses have been published, either in axisymmetric analysis (Masashi Daimaruya, 1977; Khairul Fuad, 1994) or in Cartesian coordinates (Ramachandra Rao et al. 1985 and 1988; Day. A.J, 1985; Ashworth et al. 1977). Ramachandra Rao et al. proposed a clock mechanism as a model to identify the heating and cooling that alternatively occur in the brake drum during braking.

This study reports the three-dimensional numerical analysis of thermal stresses in a brake drum of heavy commercial truck. The braking is done by two brake shoes and the heating and cooling occur alternatively in the brake drum during the brake application. A severe brake application is taken into account for the wheel load of 40 kN, and the braking is applied from a speed of 100 km/h until it stops with a deceleration of 0.5*g*.

مجلة جامعة أم القرى للهندسة والعمارة - المجلد ٤ العدد ٢ رجب ١٤٣٣هـ - ألون - ملزمة رقم ٤ وجه

FRICTIONAL HEAT FLUX

A leading and trailing shoe brake model is analyzed in this study. Heating and cooling that occur alternatively in the brake drum during braking is prescribed as a clock mechanism (Fig.1). The first heating occurs when the drum absorbs the energy input, or the frictional energy, for the time interval during which the drum moves from one end of each brake shoe to the other respective end with its varying velocity (say from point 1 to point 2 and from point 3 to point 4 which is depicted in Fig.1). At this period, cooling through convection takes place in the other parts of brake drum. In this analysis, the effect of thermal radiation during the cooling is neglected because it is too small compared to the convection effects. All parts of the brake drum are subjected to cooling at this period. As soon as this time lapses, the appropriate heat energy, the second heating, is given again, noting that the drum speed falls at the rate of $0.5g$ deceleration. Thus, heating and cooling occurs alternatively until the braking is fully terminated.

Investigation of brake thermal problems has so far been limited by a number of simplifying assumptions concerning the distribution of frictional heat generation over the friction interface and the proportions which are transferred to each part of the friction pair. In this analysis, the braking condition is considered under assumption of perfect contact between the brake shoes and the brake drum, and equal amount of generated frictional heat is distributed over the rubbing surface. The brake drum is assumed to absorb 95% of a major share of heat energy and the remainder goes into the brake shoes (Ashworth et al. 1977; Newcomb T.P., 1958-59 and 1961).

Considering about 5% of heat energy going to brake shoes, the heat flux resulting from the transformation of instantaneous kinetic energy can be written as follows

$$q = 0.95\frac{\Delta E_k}{\Delta t\, A_b} \tag{1}$$

where q is the heat flux generated on the frictional surface, ΔE_k is the alteration of kinetic energy from one edge to the other edge of brake shoe, Δt is the time interval during heating, and A_b is the area of the two brake shoes surface contacted to the drum.

TRANSIENT TEMPERATURE ANALYSIS

The three-dimensional unsteady state heat conduction equation for the transient temperature analysis in the brake drum is governed by the following equation

$$\frac{d^2T}{dx^2}+\frac{d^2T}{dy^2}+\frac{d^2T}{dz^2}=\frac{\rho c}{k}\frac{dT}{dt} \tag{2}$$

Neglecting the thermal radiation effects, the boundary surface condition can be written in the general form as

$$q = -k\frac{dT}{d\eta} - h(T - T_o) \tag{3}$$

where

ρ : Density
c : specific heat
k : thermal conductivity.
T : brake drum temperature at x,y,z,t
T_o : surrounding air temperature
t : Time
x,y,z : Cartesian coordinate
η : direction of heat flow
h : heat transfer coefficient

FINITE ELEMENT MODEL

A heavy and large brake drum of a commercial truck is considered for analysis. The temperature distribution is found by solving Eq.(3) using numerical analysis. ANSYS finite element based software is used to solve the problem. Fig.2 shows the finite element model of the brake drum with a circumferential fin near its open end.

SOLID90 is chosen as the element type since the simulation is done in three-dimensional model and temperature is the only degree of freedom. The model is meshed by using wedged hexahedral element shape with the total number of nodes is 47736. Appropriate element length is identified using trial and error method until it produces best and most consistent element shape. This process is important since the mesh pattern contributes significantly to the accuracy of the simulation result. It is finally come out with length element of 0.004 m and this value give best mesh for the model volume.

THERMAL STRESS ANALYSIS

Thermo-elasticity describes the behavior of elastic bodies under the influence of non-uniform temperature fields. It represents, therefore, a generalization of the theory of elasticity. The thermal stress may arise in a heated body either because of a non-uniform temperature distribution, or external constraints, or a combination of these causes.

The total strains at each point of the heated body are, thus, made up of two parts. The first part is a uniform expansion proportional to the temperature rise ΔT. Since this expansion is the same in all directions for an isotropic body, only normal strains and no shearing strains arise in this manner. If the coefficient of linear thermal expansion is denoted by α, this normal strain in any direction is equal to $\alpha\Delta T$.

The second part comprises the strains required to maintain the continuity of the body as well as those arising because of external loads. These strains are related to the stresses by means of the usual Hooke's law of linear isothermal elasticity. Thus, the strains are the sum of the two components and are, therefore, related to the stresses and temperature in any general form of orthogonal coordinate system as

$$\varepsilon_{ij} = \frac{\sigma_{ij}}{2\mu} + \frac{(1-2\nu)}{E}\delta_{ij}\sigma_{kk} - \delta_{ij}\alpha\Delta T \tag{4}$$

where

σ_{ij} : deviatoric stress components
σ_{kk} : hydrostatic stress components
μ : Lame's constant
ν : Poisson's ratio
E : modulus of elasticity
δ_{ij} : Kronecker deltas
α : linear thermal expansion
ΔT : temperature change

The strains are related to the displacements in the same manner as in isothermal elasticity since purely geometrical considerations are involved; in a rectangular Cartesian coordinate system the pertinent equations are as follows:

$$\varepsilon_{ij} = \begin{Bmatrix} \varepsilon_x \\ \varepsilon_y \\ \varepsilon_z \\ \gamma_{xy} \\ \gamma_{yz} \\ \gamma_{zx} \end{Bmatrix} = \begin{Bmatrix} \dfrac{\partial u}{\partial x} \\ \dfrac{\partial v}{\partial y} \\ \dfrac{\partial w}{\partial z} \\ \dfrac{\partial u}{\partial y} + \dfrac{\partial v}{\partial x} \\ \dfrac{\partial v}{\partial z} + \dfrac{\partial w}{\partial y} \\ \dfrac{\partial w}{\partial x} + \dfrac{\partial u}{\partial z} \end{Bmatrix} \tag{5}$$

where u, v, and w are the components of the displacement vector in the x, y, and z direction respectively.

RESULT AND DISCUSSION

The 3-D temperature distribution in the brake drum has been analyzed using finite element method. The analysis is performed with a number of assumptions. The drum material is made of grey cast iron A48 Class 40 that is homogenous and isotropic. The thermal properties of this material are as follows:

- Thermal conductivity, k = 51 W/m.K
- Specific heat, C_p = 550 J/kg.K
- Density, ρ = 7196 kg/m^3
- Thermal diffusivity, α = 12.89 x 10^{-6} m^2/s

The heat transfer coefficient along the interface between the surface of brake drum and surrounding air is also constant at 50 W/m^2.K. The main data for the brake drum dimensions are as follows

- Total length of brake drum = 270 mm
- Outer diameter of brake drum = 450 mm
- Inner diameter = 420 mm
- Thickness of brake drum = 15 mm
- Thickness of circumferential fin = 10 mm
- Length of circumferential fin = 20 mm
- Shoe contact angle = 100°
- Shoe width = 200 mm

The wheel load of 40 kN is taking into account and the braking is applied from a speed of 100 km/h to complete stop with a deceleration of 0.5g, and it takes 5.663 second. The initial temperature of the brake drum and surrounding air are set to be 30°C.

Fig.3 shows the profile of temperature rise of nodes *A*, *B*, *C*, and *D* during the first brake application. The effect of cyclic heating and cooling fluctuates the temperature rise of node *A* and reaches the peak temperature at the mid-time of brake application, when the time lapse is 2.85 s, and decreases afterward. The peak temperature of point *A* is about 248°C. This phenomenon is predominantly caused by the decreasing dissipated kinetic energy input with respect to time due to the decreasing of truck's speed. Furthermore, it can be considered that the heat convection into the surrounding air is greater than the dissipated kinetic energy input. On the other hand, nodes *B*, *C*, and *D* continuously increase until the end of braking. This means that the heat conduction of these nodes still advances until the braking is fully terminated.

The temperature history of the inner surface of brake drum in the course of braking is shown in Fig.4. It can be seen that the temperature rise in the frictional contact area is evenly distributed. The temperature rise at the flank of brake drum increases gradually, due to the poor heat conduction flowing to this area.

Fig.5 depicts the temperature history of the *a-a* cross-section. The steep or higher temperature gradient occurring in the thickness layer of 1.0 cm from the inner surface will cause higher thermal stress; and the maximum thermal stress occurs at the rubbing surface. Small gradient temperature is shown when the heat flows to the region of the circumferential fin.

The history of von Mises thermal stress for nodes *A, B, C,* and *D* is shown in Fig.6. The 95-MPa maximum thermal stress occurs at node *A* when the time of brake application is reaching $t = 1.32$ sec. Similar with the temperature profile, the profile of thermal stress is also fluctuating due to heating and cooling in the course of brake application. Considering the history of thermal stress, we can conclude that the highest thermal stress occurs at around one-fourth of braking time.

Fig.7 shows the von Mises thermal stress history in *a-a* cross-section in the course of braking. The circumferential fin has an effect to reduce the thermal stress and creates a significant thermal stress gradient that occurs in the region of rubbing surface having a layer thickness of 0.4 mm. It shows a good agreement with the results reported by Masashi Daimaruya et al. that the function of circumferential fin is not only to reinforce the brake drum but also to reduce the thermal stress and the effect of bell-mouthing due to thermal distortion.

CONCLUSION

The thermal stress distributions under a severe brake application have been discussed as the first step in investigating the initiation mechanism of heat cracks in the brake drum, the thermal stress distributions under a severe brake application have been discussed. A heavy and large brake drum of a commercial truck is considered and analyzed by using three-dimensional finite element method. It was found that the severe thermal environment occurred in the inner surface of brake drum will create a high thermal stress in the rubbing surface. The effect of cyclic heating and cooling fluctuates the temperature rise in the rubbing surface and reaches the peak temperature at the mid-time of brake application, and decreases afterward. The profile of thermal stress created in the brake drum also fluctuates and reaches the maximum value when the braking time is around one-fourth of the fully stopped brake application.

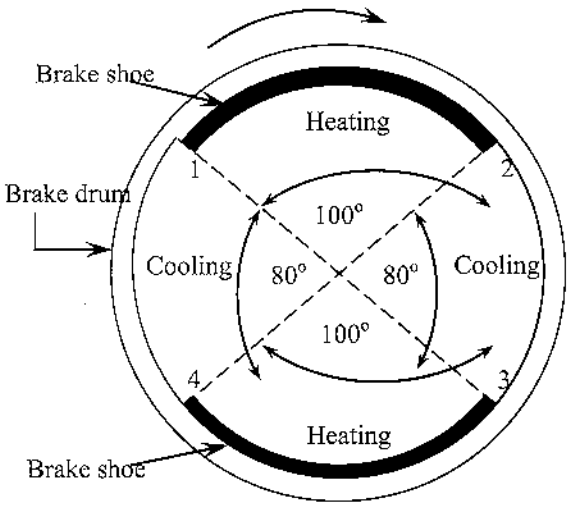

Fig.1 Clock mechanism of heating and cooling.

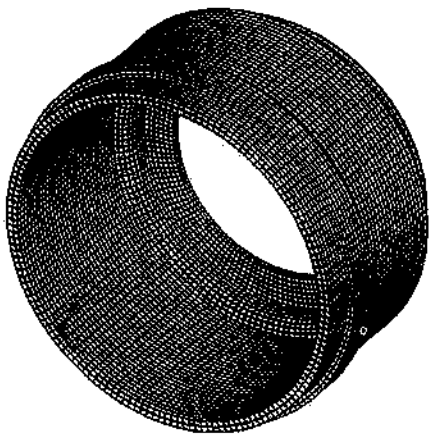

Fig.2 Meshing of finite element model.

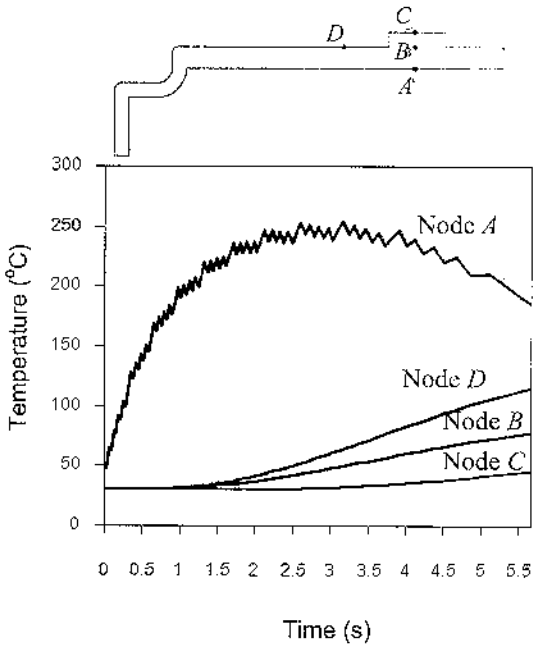

Fig.3 Temperature history of nodes *A*, *B*, *C*, and *D* at brake application.

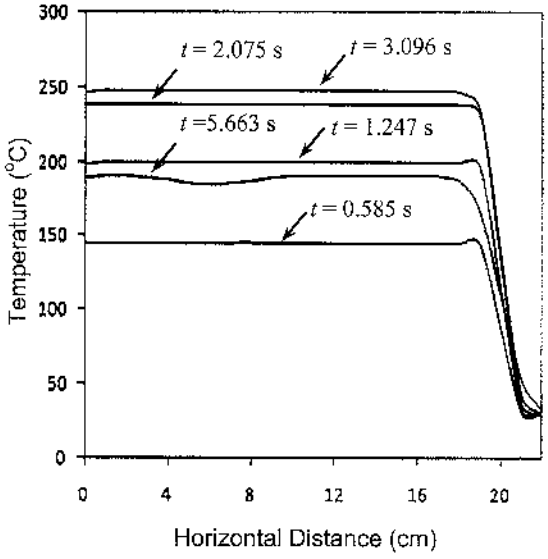

Fig.4 Temperature history of inner surface.

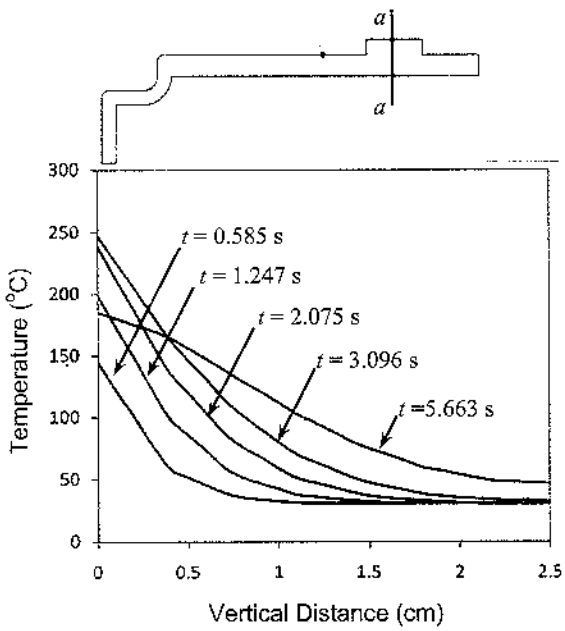

Fig.5 Temperature history of *a-a* cross-section.

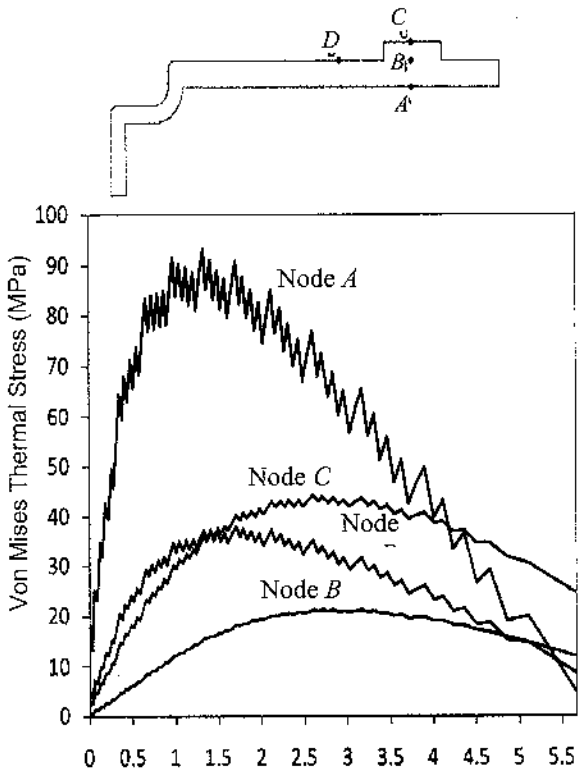

Fig.6 Thermal stress history of nodes *A*, *B*, *C*, and *D* at brake application.

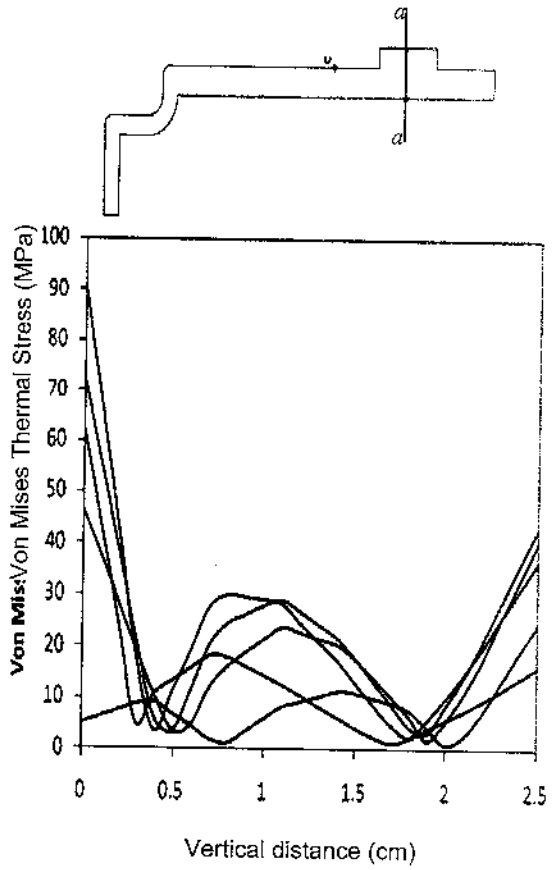

Fig.7 Thermal stress history in *a-a* cross-section.

REFERENCES

1- Khairul Fuad, Faiz Ahmad, Awaluddin Th, R.A Siregar and Alif Bin On, 2008, "Three-dimensional Analysis on Temperature Distribution in a Brake Drum of Heavy Commercial Truck, International Conference on Plant Equipment and Reliability" (*ICPER*), Paper MM-12-O, Selangor, Malaysia

2- Masashi Daimaruya, Hidetoshi Kobayashi, and Khairul Fuad, 1997, "Thermoelasto-plastic stresses and thermal distortions in a brake drum", *International Journal of Thermal Stresses*, Vol.20 (3-4), 345-361.

3- Khairul Fuad, M.Daimaruya, and H.Kobayashi, 1994, "Temperature and thermal stresses in a brake drum subjected cyclic heating, *International Journal of Thermal Stresses*, Vol.17 (4), 515-527.

4- Ramachandra Rao V.T.V.S., Ramasubramanian H., and Sheetharamu K.N., 1988, "Computer modelling of temperature distribution in brake drum for fade assessment", *Proc.Instn. Mech.Engrs*, Vol.202 (D4), 257-264.

5- Day A.J., "An analysis of speed, temperature and performance characteristics of automotive drum brakes", 1987, *ASME* No.87-Trib-11.

6- Ramachandra Rao V.T.V.S., Ramasubramanian H., and SheetharamuK.N., 1985, "Simulation of temperature distribution in drum brakes – comparison with measurements", Proceeding of *NUMETA*, Swansea, 841-849.

7- Ashworth R.J., El-Sherbiny M., and Newcomb T.P., 1977, "Temperature distribution and thermal distortions of brake drums", Proc.Istn.Mech.Engrs. (191), 169.

8- Newcomb T.P., 1961, "Interfacial temperatures and the distribution of heat between bodies in sliding contact", Int. Heat Transfer Conf. (*ASME*), 77.

9- Newcomb T.P., 1958-59, "Transient Temperatures in brake drums and linings", Proceeding Auto. Div. Instn.Mech.Engrs. (7), 227.

Received 20/9/1432;20/8/2011, accepted 25 /4 /1433; 18/3/2012

Umm Al-Qura Univ. J. Eng.& Arch. Vol. 4, No.2, pp. 37-53 (2011) 32-07-007 © The University Press 27-40

Finite Element Analysis for Molar-Tooth Treatment with Different Filler Merials

Mohammed W. Al-Hazmi
Mechanical Engineering Department,
Umm Al-Qura University
Makkah, Kingdom of Saudi Arabia
Email: mwhazmi@uqu.edu.sa

ملخص البحث

عادة ما ينتج تسوس الأسنان من الأحماض التي تنتجها البكتريا الناتجة من التفاعل الغذائي، والتي تؤدي في النهاية الى تجاويف. وتتطور هذه التجاويف تتطور إلى فتحات صغيرة، أو حفر في أعماق السن. وهي نوع شائع يتسبب في أمراض الأسنان، حيث أنها تحدث عادة على سطح السن أو التاج. وعادة ما يتعامل أطباء الأسنان مع هذه الحالات بتنظيف التسوس وعمل تجويف مناسب والاستعاضة عنها بحشوات خاصة.

وهذا البحث دراسة وتحليل لعدد من الحشوات المختلفة المستخدمة في علاج تسوس الأسنان (الضرس). وقد استخدمت نظرية العناصر المحدودة باستخدام برنامج إي-إن-إس-واي-إس (ANSYS) في هذه الدراسة، والتي يتم فيها تحليل الإجهادات على الأسنان مع حشوات مختلفة، وهي: الأملغم، والذهب، والمواد المركبة التي تستخدم في الحشوات في العيادات، ومقارنتها بالسن العادي من دون حشوة أو تجويف. وتشير الدراسة إلى أن الأملغم هو الأقرب في النتائج إلى السن العادي من دون حشوة.

ABSTRACT.

Dental caries grows by the localized dissolution of the tooth hard tissues, caused by acids that are produced by bacteria in the dental plaque on the teeth and eventually lead to "cavities". These cavities are decayed areas of the tooth that develop into tiny openings or holes, a pit and fissure cavities are the common type of tooth diseases which occurs on the chewing surface of the teeth. Dentists treated the tooth by removing the decayed tooth material with a drill and replacing it with a filler material.

This study is an investigation of the molar tooth treatment with different filler materials, amalgam, composites and gold. The analysis is completed and achieved by using finite element analysis with ANSYS software. Therefore, the results are indicating that the amalgam is the best filler material for molar tooth treatment.

Keywords:
Finite Element Analysis, Dental Analysis, Filler Material, Tooth Treatment.

1. Introduction:

Dental caries (tooth decay) is probably the most common regular diseases in the world. Although caries has affected humans since antiquity, the popularity of this disease has greatly increased worldwide now owing to food changes. Tooth decay usually occurs in children and young adults but can affect any person. The bacteria are normally present in the mouth. These bacteria convert all foods (especially sugar and starch) into acids. Furthermore, these bacteria, acid, food debris, and saliva combine in the mouth to form a sticky substance called plaque that adheres to the teeth (see Figure 1 and 2). It is most prominent on the back molars, just above the gum line on all teeth, and at the edges of fillings. Plaque that is not removed from the teeth mineralizes into tartar. Plaque and tartar irritate the gums. Plaque begins to build up on teeth within 20 minutes after eating (the time when most bacterial activity occurs). If this plaque is not removed thoroughly and routinely, tooth decay will not only begin, but also grow [1, 2, 3, 4].

The acids in plaque dissolve the enamel surface of the tooth and create holes in the tooth (cavities). Cavities are usually painless until they grow very large and affect nerves or cause a tooth fracture. If left untreated, a tooth abscess can develop. It also destroys the internal structures of the tooth (pulp) and ultimately causes the loss of the tooth [5, 6, 7].

However, there are three types of cavities. Smooth surface cavities occur on the smooth sides of the teeth, while root cavities develop on the surface over the roots. Hollow and crack cavities occur on the chewing surface of the teeth, as shown in Figure 3 & 4.

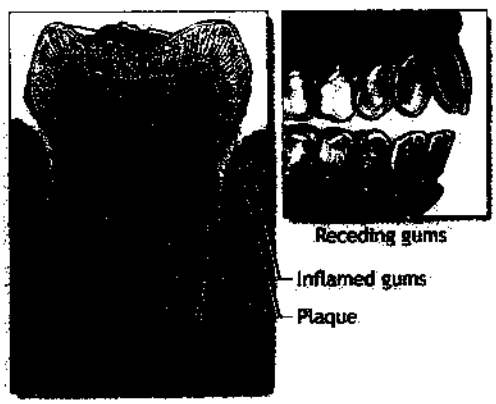

Figure 1: Plaque that adheres to the teeth

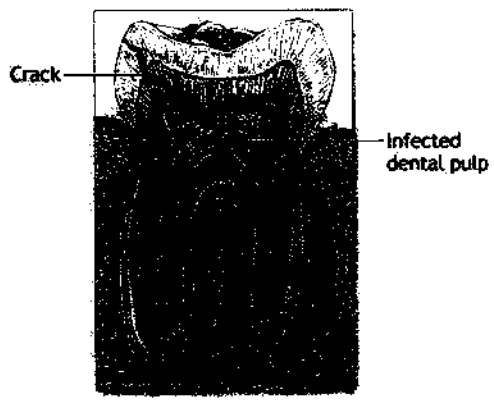

Figure 2: Infected dental pulp

Figure 3: Hollow and crack cavities

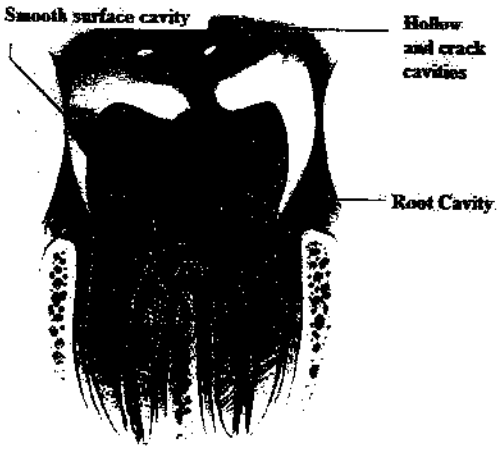

Figure 4: Types of tooth cavities

Tooth treatment can help to avoid the tooth damages from leading to cavities. Fillings, crowns and root canal are the most common type of tooth treatments. Dentists fill teeth by removing the decayed tooth material with a drill and replacing it with a material such as gold, silver amalgam alloy, or composite resin. Composite resin more closely matches the natural tooth appearance, and may be preferred for front teeth. Many dentists consider silver amalgam (alloy) and gold to be stronger, and these materials are often used on back teeth. There is a trend to use high strength composite resin in the back teeth as well [8, 9].

Crowns, or "caps" are used if tooth decay is extensive and there is limited tooth structure, which may weaken teeth. Large fillings and weak teeth increase the risk of the tooth breaking. The decayed, or weakened area is removed and repaired. A crown is fitted over the remainder of the tooth. Crowns are often made of gold, porcelain, or porcelain attached to metal [10, 11].

A root canal is recommended if the nerve in a tooth dies from decay or injury. The center of the tooth, including the nerve and blood vessel tissue (pulp), is removed along with decayed portions of the tooth. The roots are filled with a sealing material. The tooth is filled, and a crown may be placed over the tooth if needed, Figure 5 shows tooth structure includes dentin, pulp and other tissues, blood vessels and nerves imbedded in the bony jaw [12].

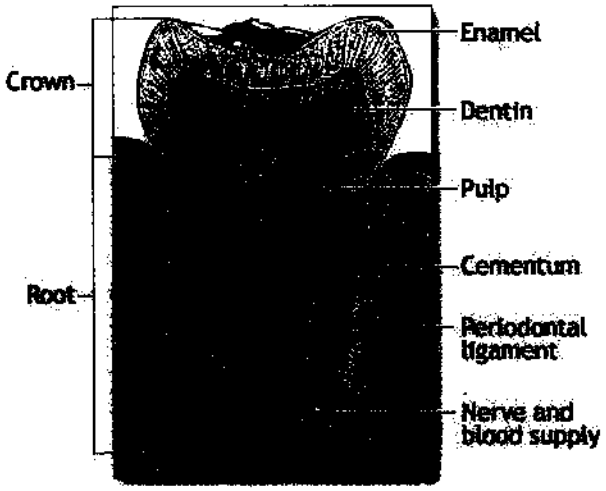

Figure 5: Tooth anatomy

However, many studies on filler composition and polymerization methodology for composite materials have resulted in both increased esthetic qualities and resistance to wear. Similarly, the benefits of sealants are becoming more widely accepted for the prevention of hollow -and-fissure caries.

Further research on biomaterials has led to the introduction of vastly improved dental materials. Developments in impression materials and gold foil and advancements in knowledge about liners and sealers are also factors that have resulted in better care and treatment for patients. Advances in metallurgy have resulted in a variety of improved alloys that are either already available, or are being developed. Corrosion-resistant amalgam alloys have been developed, which will enhance the oral health of the population by providing longer lasting restorations [12,13].

2. Filler Materials:

In this study, there are three different filler materials used for molar tooth treatment: dental amalgam, gold and composites [14:18]:

2.1. Dental Amalgam

Amalgam technically means an alloy of mercury (Hg) with any other metal. Dental amalgam is an alloy made by mixing mercury with a silver-tin dental amalgam alloy (Ag-Sn), see Table 1.

2.2. Direct-Filling Gold

Gold is extremely soft and may be welded to itself under pressure at room temperature if the surfaces being fixed and cleaned. This makes gold applicant to a direct restoration. Although it has been used this way for more than a century, the process is tedious, difficult, and relatively expensive for the patient.

Gold for direct-filling restorations may be classified on the basis of (1) the geometric form in which it is supplied; (2) the surface condition of the part; and (3) the microstructure of the part. It may be supplied as ropes, sheets, strips, or pellets. Direct gold is essentially 100% gold. Pre-alloying with other elements would reduce the weldability and malleability at room temperature. However, other elements may incorporate (platinum or calcium) indirectly into the final structure by layering them onto the gold in form such as gold foils. During cold welding, much greater compaction pressures are required to remove pores or spaces in mat gold and powdered gold than in gold foil.

2.3. Composites

A composite is a physical mixture of materials. The parts of the mixture are generally chosen with the purpose of averaging the properties of the parts to achieve intermediate properties. Quite often, a single material does not have the appropriate properties for a specific dental application. Composites typically involve a dispersed phase of filler particles distributed within a continuous phase (matrix phase). In most cases, the matrix phase is fluid at some point during the manufacture or fabrication of a composite system. A dental composite has traditionally indicated a mixture of silicate glass particles within an acrylic monomer polymerized during the application. The silicate particles provide mechanical reinforcement of the mixture (reinforcing fillers) and produce light transmission and light scattering that adds enamel like transparency to the material. The acrylic monomers make the initial mixture fluid and moldable for placement into a tooth preparation. The matrix flows to adapt to tooth preparation walls and penetrate into micromechanical spaces on etched enamel or dentin surfaces.

3. Background of Molar Tooth Analysis Using FEM:

Several studies for tooth analysis using FE method such as *(Genovese, et al, 2004)* [19] investigated the mechanical behavior of a new customized post system built up with a composite framework presently utilized for crowns, bridges, veneers and mainly only dental restorations. The material has been shaped so as to follow perfectly the profile of the root canal in order to take advantage of the better mechanical properties of composites with respect to metallic alloys commonly used for cast posts. The analysis has been carried out with 3-D finite element models previously validated on the basis of experimental work. The new post system has been compared to a variety of restorations using either prefabricated or cast posts. The structural efficiency of the new restoration has been evaluated for an upper incisor under different loading conditions (mastication, bruxism, impact).

Results prove that maximum stress values in restored teeth are rather insensitive to post types and materials. However, the new customized composite restoration allows to reduce significantly the stresses inside the dentinal regions where conservative clinical interventions are not possible.

Pattijn, et al, (2005) [20] evaluated the modal behavior of the bone–implant–transducer (Osstell) system by means of finite element analyses. The influence of different parameters was determined: (1) the type of implant anchorage being trabecular, cortical, uni-cortical, or bi-cortical; (2) the implant diameter; (3) the length of the implant embedded in the bone; and (4) the bone stiffness.

The type of anchorage determines the resulting modal behavior of the implant–transducer system. A rigid body behavior was found for a uni-cortical anchoring and homogeneous anchoring with low bone stiffness (≤1000 MPa), whereas a bending behavior was found for a homogeneous anchoring with a high bone stiffness (≥5000 MPa) and bi-cortical anchorage. The implant dimensions influence the values for the resonance frequencies. Generally, an increase in implant diameter or implant length (in bone) results in higher resonance frequencies. Their study also showed that resonance frequencies in case of rigid body behavior of the implant–transducer system are more sensitive to changes in bone stiffness than resonance frequencies in case of bending behavior. In conclusion, it seems that the Osstell transducer is suited for the follow-up in time of the stability of an implant, but not for the quantitative comparison of the stability of implants [20].

DeHoff, et al, (2004) [21] studied the viscoelastic option of the ANSYS finite element program to calculate residual stresses in an all-ceramic FPD for four ceramic–ceramic combinations. A three-dimensional finite element model of the FPD was constructed from digitized scanning data and calculations were performed for four systems: (1) IPS Empress 2, a glass-veneering material, and Empress 2 core ceramic; (2) IPS ErisTM a low fusing fluorapatite-containing glass-veneering ceramic, and Empress 2 core ceramic; (3) IPS Empress 2 veneer and an experimental lithium–disilicate-based core ceramic; and (4) IPS ErisTM and an experimental lithium–disilicate-based core ceramic. The maximum residual tensile stresses in the veneer layer for these combinations were as follows: (1) 77MPa, (2) 108MPa, (3) 79 MPa, and (4) 100MPa. These stresses are relatively high compared to the flexural strengths of these materials. In all cases, the maximum residual tensile stresses in the core frameworks were well below the flexural strengths of these material. They concluded that the high residual tensile stresses in all-ceramic FPDs with a layering ceramic may place these systems in jeopardy of failure under occlusal loading in the oral cavity [22].

Ueda, et al, (2004) [23] investigation used the comparison of photoelastic analysis, the stress distribution in a fixed prosthesis with 3 parallel implants, to the stress distribution in the same prosthesis in the existence of an angled central implant. Two photoelastic resin models were made and a polariscope was used in the visualization of isochromatic fringes formed in the models when axial loads of 2 kg, 5 kg and 10 kg were applied to a unique central point of the prosthesis. The presence of inducted tensions (preloads) was observed in the models after applying torque to the retention screws. Preloads were intensified with the incidence of occlusal forces. In the parallel implants, the force dissipation followed the long axis. The angled implant had a smaller quantity of fringes and the stresses were located mostly around the apical region of the lateral implants.

A 3-D solid model of a human maxillary premolar was prepared and exported into a 3-D-finite element model (FEM) by *Ausiello, et al,* (2001) [24] and a generic class II MOD cavity preparation and restoration was simulated in the FEM model by a proper choice of the mesh volumes. A validation procedure of the FEM model was executed based on a comparison of theoretical calculations and experimental data. Different rigidities were assigned to the adhesive system and restorative materials. Two different stress conditions were simulated: (a) stresses arising from the polymerization shrinkage and (b) stresses resulting from shrinkage stress in combination with vertical occlusal loading. Three different cases were analyzed: a sound tooth, a tooth with a class II MOD cavity, adhesively restored with a high (25GPa) and one with a low (12.5 GPa) elastic modulus composite.

The cusp movements induced by polymerization stress and (over)-functional occlusal loading were evaluated. While cusp displacement was higher for the more rigid composites due to the prestressing from polymerization shrinkage, cusp movements turned out to be lower for the more flexible composites in case the restored tooth which was stressed by the occlusal loading.

This preliminary study by 3-D FEA on adhesively restored teeth with a class II MOD cavity indicated that Young's modulus values of the restorative materials play an essential role in the success of the restoration. Premature failure due to stresses arising from polymerization shrinkage and occlusal loading can be prevented by proper selection and combination of materials [25].

Ghulman and Al-Hazmi (2008) [26] investigated the stress analysis of the molar tooth under loading conditions with different angles, using finite element package ANSYS. The results of their study indicated that the maximum shearing stress and deformation ~~is~~ increases with decreasing directional angle of the applied load.

The objective of this study is to investigate the stresses and deformations in proximal dentine of human molar-tooth with different filler materials. A finite element model of molar-tooth was constructed, based on a 3-D solid modeling using AutoCAD and exported to ANSYS FE software to calculate the stress deformation distributions on the molar tooth with different filler materials which are implemented in a cavity, located in the middle of the tooth crown.

4. Finite Element Modeling for Molar-Tooth

The approach in this study is to model the molar-tooth by using the 3D finite element modelling capabilities of ANSYS with cavity located in the central part of the tooth crown. In this FE analysis, different filler materials are added to the tooth cavity.

4.1. Molar-tooth Geometrical Model and Boundary Conditions:

Two steps were used for modeling the molar-tooth. First, a 3-D solid modeling is constructed using AutoCAD with a cavity at the top center of the tooth crown, as shown in Figure 6. Subsequently the model is exported to ANSYS for FE Analysis.

Figure 7 (a&b) shows the molar-tooth modelling by ANSYS. The 3-D element SOLID92 with 6 degree of freedom is used for modelling the molar-tooth. The molar-tooth geometry was meshed to 423693 elements as shown in Figure 7(a).

The boundary conditions of the molar-tooth are:

Displacements in all three directions of the coordinate axes are zero at the roots of the tooth, as illustrated in Figure 8: $U_x = U_y = U_z = 0$.

Also rotations about all three coordinate axes are zero at the roots of the tooth, as shown in Figure 8: $Rot_x = Rot_y = Rot_z = 0$.

Figure 6: 3-D soled model of molar-tooth

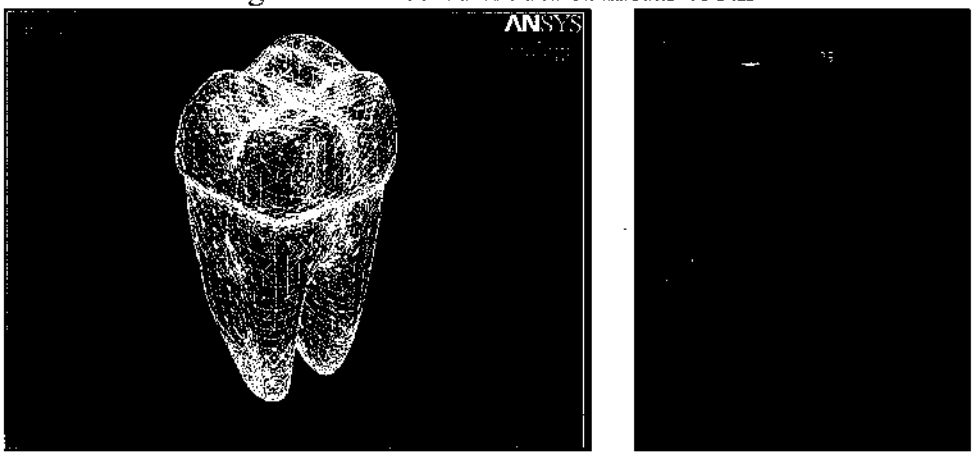

a: 3-D finite element meshed molar-tooth model b: 3-D molar tooth with filling material

Figure 7: 3-D Finite element modelling of molar-tooth with filler material

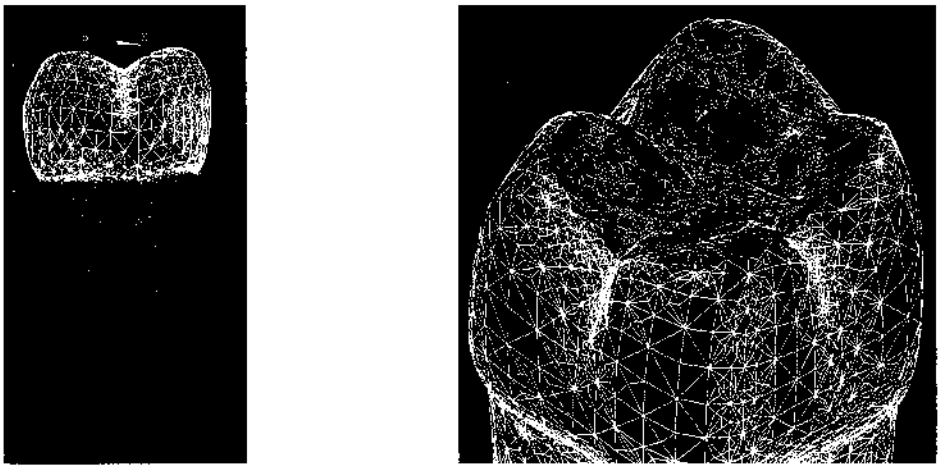

Figure 8: Boundary conditions for molar-tooth

4.2. Physical Properties

Table 1 gives the physical properties for the different materials:

Table 1: Material properties [*Genovese, et al (2004), and Lee, et al, (2002)*]

Material	Yield modulus E (MPa)	Possion ratio's ν
Enamel	84100	0.20
Dentine	18600	0.31
Pulp	2	0.45
Amalgam	27600	0.35
Gold (alloy)	99300	0.3
Composite alloy	218000	0.35

5. Results and Discussion:

The results are presented for, molar-tooth cavity treated with three different filler materials (Amalgam alloy, composites, and gold) applied pressure over the top surface of molar tooth crown with 100 N/mm^2.

Molar- tooth without cavity (natural tooth):

Figure 9 (a & b) shows the finite element results of the molar-tooth deformation and maximum shear stress profiles. The results show that the maximum deformation is 0.362967 mm at the top surface of the molar tooth and maximum shear stress is 7590. MPa at the top surface of the molar-tooth.

Molar-tooth with Amalgam filler material:

Figure 10 a & b shows the finite element results of the molar-tooth with cavity treated by amalgam filler material. The results show that the maximum deformation is 0.352621 mm at the top surface of the tooth and maximum shear stress is 7510 MPa at the top surface of the tooth. The results indicate that the total deformation of the molar-tooth with filler of amalgam material is less than the total deformation of the molar-tooth without filler, and the maximum shear stress of on the molar-tooth with filler of amalgam material is less than the molar-tooth without cavity at similar conditions.

Molar-tooth with gold filler material:

Figure 11 a & b shows the finite element results of the molar-tooth with a cavity treated by gold filler material. The results show that the maximum deformation is 0.325829 mm at the top surface of the tooth and maximum shear stress is 7270 MPa at the top surface of the tooth. The results indicate that the total deformation of the molar-tooth with a filler of gold material is less than the total deformation of the tooth with a filler of amalgam material, and the maximum shear stress on the molar tooth with a filler of gold material is less than the molar-tooth with a filler of amalgam material at similar conditions.

Molar-tooth with composite filler material:

Figure 12 a & b shows the finite element results of the molar-tooth with a cavity treated by composite filler material. The results show that the maximum deformation is 0.315388 mm at the top surface of the tooth and maximum shear stress is 7225 MPa at the top surface of the molar-tooth. The results indicate that the total deformation of the molar-

tooth with composite filler material is less than the total deformation of the tooth with a filler of gold and amalgam material, and the maximum shear stress of on the molar tooth with filler of composite material is less than the molar tooth with a filler of gold and amalgam material at similar conditions.

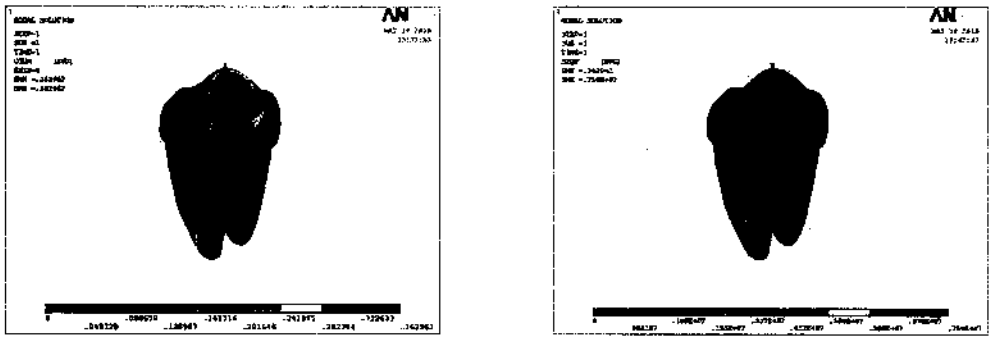

(a) Total deformation of the molar tooth (b) Von Mises stress of the molar tooth

Figure 9: A finite element results for molar-tooth without cavity

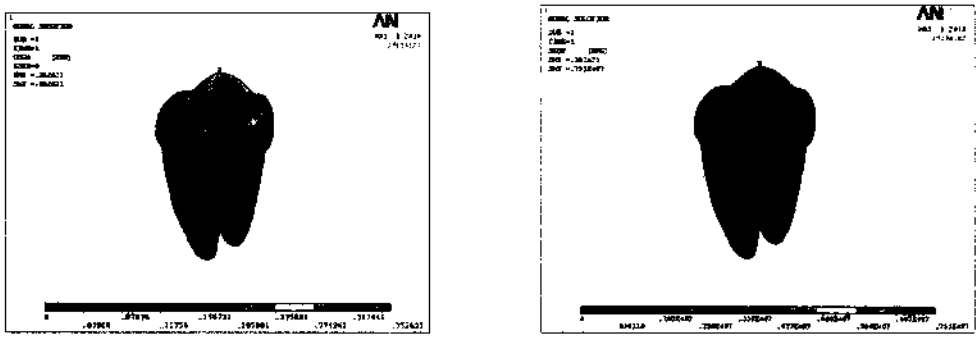

(a) Total deformation of the molar tooth (b) Von Mises stress of the molar tooth

Figure 10: A finite element results for molar-tooth with amalgam filler material

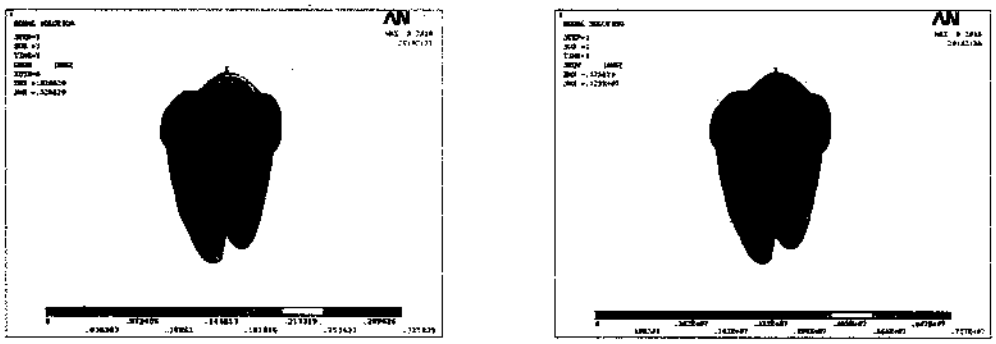

(a) Total deformation of the molar tooth (b) Von Mises stress of the molar tooth

Figure 11: A finite element results for molar-tooth with gold filler material

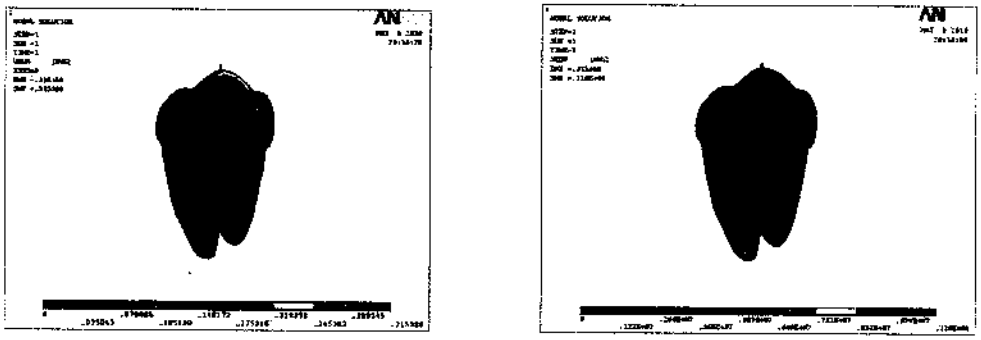

(a) Total deformation of the molar tooth(b) Von Mises stress of the molar tooth

Figure 12: A finite element results for molar-tooth with composite filler material

5. Comparison between the molar tooth and filler materials:

Figures 13, 14, 15 and 16 show a graphical evaluation of molar-tooth without a cavity, and with a cavity filled with different filler materials (amalgam, gold, and composite) alongside the molar-tooth and cross over the crown part of the molar tooth. The results indicate that the total deformation across the molar tooth is higher at molar tooth without a cavity than the tooth with filler material. As that it, increases with amalgam to gold and it decreases with composite to gold as shown at Figure 13. Furthermore, the maximum shear stress is almost similar at molar tooth without a cavity as molar tooth with amalgam filler material. However, the maximum shear stress is not quite less than the tooth with amalgam filler material as the filler with gold and composite materials, as shown in Figure 14.

Figure 15 shows the total deformation along the molar tooth. The results indicate that the total deformation at the crown part of the molar tooth is higher than the tooth with filler material. Besides that, it increases more with amalgam than gold, and decreases more with composite than gold. On the other hand, the von Mises stress (Figure 16) is the lowest at molar tooth without cavity than molar tooth with filler materials. In addition, the von Mises stress increases with filler treatment, whereas the molar tooth with composite filler is higher than the molar tooth with amalgam and gold.

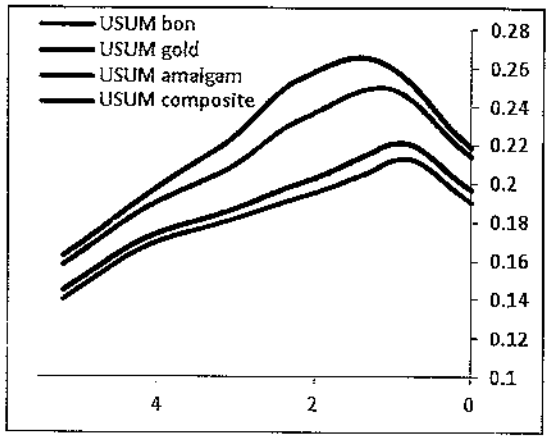

Figure 13: Total deformation of molar tooth relations across the crown

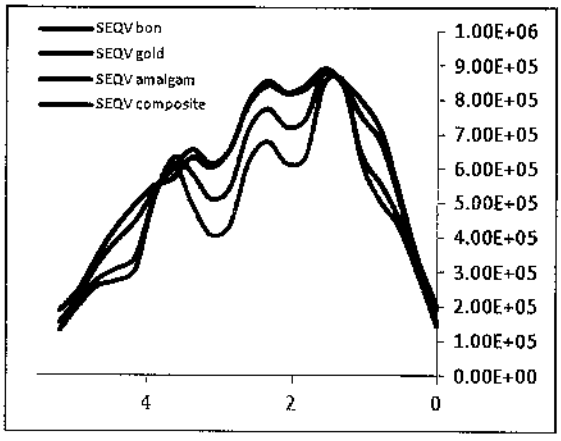

Figure 14: von Mises stress of molar tooth relations across the crown

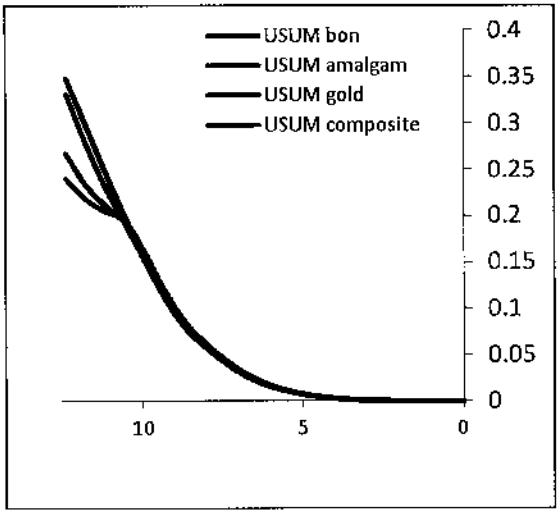

Figure 15: Total deformation of molar tooth relations along the molar tooth

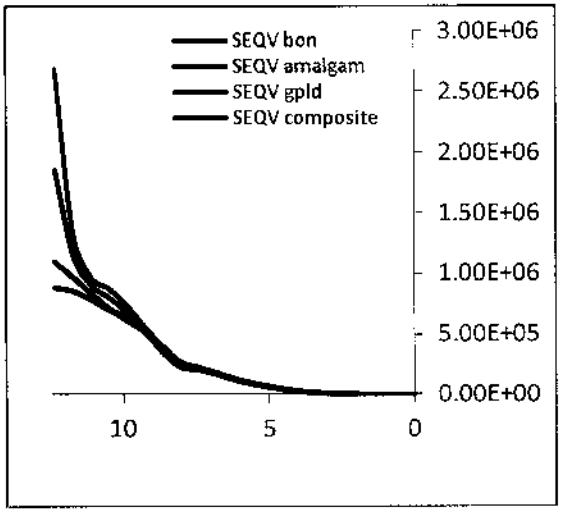

Figure 16: Von Mises stress of molar tooth relations along the molar tooth

6. Conclusion and Recommendations

This study presents a finite element analysis of the molar-tooth cavity treated with different filler materials to identify the stresses and deformations.

The results are represented in terms of maximum shear stress and total deformation for the molar tooth cavity treated with three types of filler materials (amalgam, gold, and composite). The results indicate that the maximum shear stress is the lowest with composite filler material, and increases with gold filler, amalgam filler and without cavity respectively. The total deformation is the lowest with composite filler. However, the total deformation increases with gold filler, amalgam filler, and the tooth without cavity respectively. Thus, the filler treatment with amalgam material is closer to that for the normal molar tooth without cavity. Therefore, the amalgam filler material is approximately more appropriate filler material than the gold and composite filler materials.

6.1. Recommendation for Future Work

There are several areas where more work is needed for analysis of molar-tooth. Among these studies are:

1- The study of another type of tooth treatment such as root canal tooth treatments.

2. Finite element analysis of tooth implementation.

3- The study and evaluation of molar-tooth treatment with different filler materials in order of thermal variation.

References:

1. *American Dental Association: Dentist's desk reference: materials, instruments, and equipment*, ed. 1, Chicago, 1981, American Dental Association.
2. Hillman JD, Dzuback AL, Andrews SW., "Colonization of the human oral cavity by a Streptococcus mutans mutant producing increased bacteriocin". J Dent Res 66(6):1092-1094, 1987.
3. Silverstone LM et al: *Dental Caries*, NewYork,1981, Macmillian.
4. Morin DL, Cross M, Voller VR, Douglas WH, DeLong R., "Biophysical stress analysis of restored teeth: modelling and analysis". Dental Materials, 1988;4:77-84.
5. Mondelli J, Steagall L, Ishikiriama A, Navarro M, Soares FB., " Fracture strength of human teeth with cavity preparations". J Prosthet Dent, 1980;43:419-422.
6. Niek De Jager, P.P., Albert J. Feilzer, "Finite element analysis model to simulate the behavior of luting cements during setting". Dental Materials, 2004: 1–8.
7. Beiswanger BB, "The clinical validation of early caries detection methodologies. In: Stookey GK, ed.: *Early Detection of Dental Caries*. Proceedings of the 1ST Annual Indiana Conference. Indianapolis, 1996, Indiana University School of Dentistry.
8. Elderton RJ., "Longitudinal study of dental treatment in the general dental service in Scotland". Brit Dent J 155:91-96,1983.
9. Hansen AR, Asmussen E, Christiansen NC., " In vivo fractures of endodontically treated teeth restored with amalgam". Endod Dent Traumatol, 1990;6:49-55.
10. R.C. Atwooda, P.D.L., , R.V. Curtis, "Modeling the surface contamination of dental titanium investment castings". Dental Materials, 2005. 21: p. 178–186.
11. Ralf J. Radlanski, H.R., "Explainable and critical periods during human dental morphogenesis and their control". Archives of Oral Biology, 2004. 50: 199—203.
12. Kraus BS, Jordan RE, Abrams L., "Dental anatomy and occlusion". ed. 1, Baltimore, 1969,Williams & Wilkins.
13. Hausen H., "Caries prediction-state of the art". Community Dent Oral Epidemiol 25:87-96, 1997.
14. Mondelli J, Steagall L, Ishikiriama A, Navarro M, Soares FB., " Fracture strength of human teeth with cavity preparations". J Prosthet Dent, 1980;43:419-422.
15. Craig RG, Powers JM, Wataha JC., "Dental materials: properties and manipulation", ed 7, St Louis, 2000, Mosby.
16. Craig RG., *Restorative Dental Materials*. ed. 11, St Louis, 2001, Mosby.
17. Ferracane JL,. *Materials in Dentistry-Principles and Applications*". Philadelphia, 1995, JP Lippincott.
18. Chris Ford , Xiao-Zhi Hu, Hong Zhao, "A numerical study of fracture modes in contact damage in porcelain/Pd-alloy bilayers". *Materials Science and Engineering*, 2003: 202–206
19. K. Genovese , C. Pappalettere, "Finite element analysis of a new customized composite post system for endodontically treated teeth". *Journal of Biomechanics*, 2004.
20. V. Pattijn, C.V.L., G. Van der Perrea, I. Naertc, J. Vander Sloten, "The resonance frequencies and mode shapes of dental implants: Rigid body behaviour versus bending behavior". A numerical approach. *Journal of Biomechanics*, 2005.
21. Paul H. DeHoff , K.J.A., Nils Götzen, "Viscoelastic finite element analysis of an all-ceramic fixed partial denture". *Journal of Biomechanics*, 2004.
22. Pashley DH., "The effects of acid etching on the pulpodentin complex". Operation Dent 17(6):229-242,1992.

23. Cristiane Ueda, R.A.M., Cláudio Luiz Sendyk, Dalva Cruz Laganá, "Photoelastic analysis of stress distribution on parallel and angled implants after installation of fixed prostheses". Braz Oral Res, 2004. 18(1): 45-52.
24. P. Ausiello, A.A., C.L. Davidson, S. Rengo, "3D-fnite element analyses of cusp movements in a human upper premolar, restored with adhesive resin-based composites". Journal of Biomechanics, 2001: 1269–1277.
25. Pietro Ausiello , S.R., Carel L. Davidson, David C. Watts,. "Stress distributions in adhesively cemented ceramic and resin-composite Class II inlay restorations: a 3D-FEA study". Dental Materials, 2004. 20: 862–872.
26. Hamza A. Ghulman, Mohammed W. Al-Hazmi, "Finite Element Analysis for Molar-Tooth under Different Loading Conditions". *Mansoura Engineering Journal*, December 2008, Pages M 57-M68.

Received 10/7/1432;12/6/2011, accepted 25 /4 /1433; 18/3/2012

Umm Al-Qura Univ. J. Eng.& Arch. Vol. 4, No.2, pp. 37-53 (2011) 32-04-003 © The University Pres s41-58

The Effect of the Manufacturing Errors on the Dynamic Performance of Gears

M. W. AL-HAZMI[1]

[1)] Mechanical Engineering Dept. College of Engineering and Islamic Architecture , Umm Al-Qura University, Makkah, KSA.

تأثير عيوب التصنيع على الأداء الديناميكي للتروس

الخلاصة:

تعتبر التروس من أكثر العناصر الميكانيكية المستخدمة لنقل القدرة في المعدات الدوارة. كما أن تحليل إشارات الاهتزازات الصادرة منها تعتبر من أهم معايير الحكم على أداء هذه المعدات. إلا أن هذه الإشارات غالبا ما تكون معقده ومركبة نظرا لاحتوائها على ترددات مركبة تمثل جميع عناصر التروس قيد الدراسة. وقد تعددت الأبحاث السابقة والأساليب المتنوعة في هذا المجال بهدف استخلاص البيانات المطلوبة لتشخيص أعطال التروس. وقد أجمع الباحثون أن هذه الأساليب لا تزال تحتاج إلى تبسيط بغية تسهيل استخلاص البيانات المطلوبة لتشخيص الأعطال.

ولهذا فإن البحث الحالي يهدف إلى إيجاد علاقات مبسطه تربط بين عيوب تصنيع التروس وأعطالها وبين الأداء الحركي لها. ولتحقيق هذا الغرض، تم تصميم مجموعة أزواج من التروس، بالإضافة إلى صندوق تروس، بحيث يصبح التحكم في المسافة بين محاور التروس ممكناً لدراسة تأثير عيوب التروس والتركيب على الأداء الحركي. وقد أوضحت النتائج أن الإشارات المسجلة في النطاقين الزمني والطيفي مفيدة في تشخيص أعطال التروس.

ABSTRACT

Gears are among the most common mechanisms used in mechanical applications. Vibration signals acquired from a gearbox are usually complicated, due to the existence of different frequencies generated by modulation. Consequently, vibration signals are often containing dynamic information for fault diagnosis and prediction of failure. Several techniques such as FFT frequency spectrum, Cepstrum analysis, Envelope Analysis, as well as Hilbert transform, and others are applied to analyzing gear vibration signals to extract the gear fault.

The aim of the present work is to simplify the correlation between the main gear manufacturing errors and their dynamic response signals. For this reason, damages in gear tooth and error in center distance between gears were investigated. The results show that, the vibration time signals as well as the frequency response signal were useful for analyzing the fault diagnosis of gears.

KeyWords:

Gear dynamics – Vibration – Severity vibration – Envelope Analysis – Frequency Spectrum – Gear Errors

1. INTRODUCTION

Gears are one of among the most common mechanisms used for transmitting power and motion in numerous mechanical applications. Previous studies on gear teeth contacts have been considered as one of the most complicated applications. Good understanding of vibration signals is required for the early detection of incipient gear failure to achieve high reliability. Vibration signals acquired from a gearbox are usually complicated to predict the symptoms of an inherent fault due to the existence of meshing frequencies, their harmonics, and coupled frequencies generated by modulation. Cepstrum analysis calculation can be performed on FFT spectrum or envelope spectrum, and has a simplification of the analysis of vibrations of gearboxes, which are extremely difficult to analyze. Envelope Analysis of the FFT frequency spectrum of the modulating signal is useful technique for extracting the modulating signal from an amplitude-modulated signal [1]. Vibration signals from a gearbox are usually noisy and the signal-to-noise ratio is low, so that feature extraction of signal components is very difficult. A new noise canceling method, based on time-averaging method, is developed by M.A. Jafarizadeh, et al [2] in which feature extraction and diagnosis of different gear damages are designated.

Hilbert transform, wavelet packet transform (WPT) and empirical mode decomposition (EMD) are applied to gear vibration signals to extract the fault characteristic information [3,4]. EMD is a method of breaking down a signal for system excited due to gear errors and profile modifications. EMD gives early detection of pitting [5-7]. The wavelet transform (WT) is suitable to represent all possible types of transients in vibration signals generated by faults in a gear box [8]. Moreover, the vibration signal of a spur bevel gear box in different conditions is investigated using discrete wavelets [8,9]. X. Fan and M. J. Zuo [10] proposes a new fault detection method that combines Hilbert transform and wavelet packet transform. Both simulated signals and real vibration signals are collected from a gearbox dynamics simulator which shows that the proposed method is effective to extract modulating signal and help to detect the early gear fault. More features are extracted from vibration signals and fed to a fuzzy classifier which is built and tested with representative data. The results are found to be encouraging [11]. As compared to the wavelet transform, the multiscale statistical scheme is an attractive option due to its low complexity, high sensitivity and inherent robustness [12]. A simple technical diagnostic feature is based on the fact that, a gearbox in a bad condition, is more susceptible to load than the gearbox in a good condition, and the relation will be different [13]. A mathematical model is proposed to describe the mechanisms leading to modulation sidebands of planetary gear sets. This model is used to demonstrate modulation sidebands from acceleration measurements [14,15].

Differences in gear materials, material processing, and gear operating properties may significantly affect the amounts of such plastic deformations before tooth breakage [16]. While, the effect of common tooth faults: spalling and breakage, bending, fillet foundation and contact deflection are analytically computed by using analytical gearmesh issued from analytical modeling and the vibration signatures [17]. The growth in a tooth crack is reflected in the total mesh stiffness of the gear system [18]. A simulation model for producing typical fault signals from gearboxes is tested as a new diagnostic algorithms, and possibly prognostic algorithms [19-20]. Modal testing experiments presented by M. Amarnath [21] and J. Hongkai, et al [22] have been carried out on the gear starting from healthy to worn out conditions to quantify wear damage. The results provide good

understanding for vibration parameters as measures for effective assessment of wear in spur gears. Signal processing tools, based on the Order Tracking Method, were developed by Jean-Luc Dion, et al [23], in order to clarify the underlying phenomena involving gear impacts. From the aforementioned and other researches, the analysis of gear signals still need more intensive work and easier techniques for understanding gear fault diagnosis.

Therefore, the aim of the present work is to simplify correlation between the main gear manufacturing error and the measured dynamic response signals. These correlations may be useful to study and analyze both time and frequency response spectra of vibration generated from meshing gears. For this reason, damages in gear tooth and error in center distance between gears are usually investigated for both straight spur and helical gear.

2. INSTRUMENTATION OF THE EXPERIMENTAL WORK

2.1 Tested Gear Unit.

In this work, the effect of tooth damages and error in manufacturing gear teeth. Also, the effect of changing the center distance of the meshed gears were investigated. For this purpose, four pairs of gears were designed and manufactured for representing versatile single stage gearbox. The first two pairs were made of steel gears having straight spur teeth; one pair had correct teeth while the other pair had deliberated damage in one tooth as shown in Fig.1. For the sake of comparison, the other two pairs were made of the same material but with helical teeth. The helical teeth were designed and manufactured with the same center distance as the spur gear. Similarly, one pair contains correct teeth, while the other is with deliberated damaged tooth. There are three experimental test has been done to examine, two correct gears, one correct gear meshed with another gear with damaged tooth, and finally two gears, both of which with damaged tooth. All experiments were carried out either on spur gears or helical gears. Both types of gear were designed with transmission ratio of (3), number of teeth (25/75) and module of 2mm. All pairs have the same center distance 101.543mm pressure angle of 20°, while the helical gears were designed with helix angle of 10°. The center distance of the spur gears was kept the same by shifting the teeth profile of the spur gear. Moreover, the influences of backlash or setting errors in the center distance of gears were also investigated for both types of gears. In order to simulate gear boxes with different errors in center distance, the bearing location of one shaft must be changed. For this purpose, the bearings of the output shaft are mounted in the housing of special design. These bearing housings were equipped with eccentric bores which allow changes in bearing position if the housing is rotated. Fig.2 shows a bearing housing with eccentric bore divided on the other face with angular scale related to the shift in position. The relation between the angular position of the bearing housing and the value of change in center distance are shown in Table 1. The eccentric bore allows the center distance to be changed from -0.45mm to +0.904mm. The positive value means excessive clearance or backlash, while the negative value means interference between gear teeth. Additional work was carried out to study the dynamic performance of gears under two different working conditions, loaded or unloaded. A standard braking unit was used to apply a resisting torque on the output shaft. The applied braking torque was calculated using FEA to find out the maximum permissible value at which gear failure will not occur.

2.2 Measurements of Rotating Speeds:

High precise speed control unit was chosen to control both direction and speed of the driving motor. Running speed at 1800 rpm was selected to carry out the whole experimental tests. Based on the selected speed, the input shaft runs at 30 Hz (1800rpm/60), while the output shaft runs at 10 Hz (30Hz/ speed ratio (3)). Gear meshing frequency is calculated by [pinion speed (30 Hz) multiplied by the number of its teeth (25)] or equal to [gear speed (10 Hz) multiplied by its teeth (75)] which is equal to 750Hz. Moreover, during testing gears with damaged teeth, the direction of rotation was, therefore, important. Precisely, the rotating speed of the input shaft of the gearbox was measured using photoelectric tachometer. The tachometer output signal was fed to the computerized interface system analyzer to work as reference signal for the measuring spectrum.

2.3 Vibration Measurements

In this analysis, an interface analyzer is used to measure the vibration signals with different parameters and forms. As shown in Fig. 3 the vibration signal can be measured using two channels vibration analyzer. Two identical vibration sensors (accelerometers) can be mounted in vertical or horizontal position. During tests, the vibration sensors were mounted on the rigid location of the bearings to avoid the effect of the housing resonance. The output signals of the sensors have been pre-processed, using signal amplifier, and fed to the computerized analyzer to be presented in time domain. Furthermore, processing had been carried out to transfer the acquired signals from time domain to frequency domain, using FFT technique. Moreover, other developments can be carried out to extract the modulating signal using envelope analysis technique. Most of the vibration measurements were recorded for spur toothed gear with correct teeth, with damaged small gear (pinion), with damaged large gear, and both gears were with damaged teeth. The same procedure was repeated for helical gears and during changing the center distance between gears.

2.3.1 Measurements of vibration Severity:

It is well-known that the vibration severity of the time domain vibration signals is a good indicator for the overall vibration level, or the global performance of the investigated system. Usually, the vibration severity is represented in one value and can be measured in different forms, such as displacement (micron), velocity (mm/sec) or acceleration (m/sec^2).

2.3.2 Measurements of Frequency Response Spectra:

For detailed analysis, the response signals in time domain were transformed to frequency domain using FFT method. The vertical axis of the frequency spectra may be presented in different parameters such as velocity or acceleration. Moreover, zoom in/out are additional facilities for detailed investigations which mainly depend on the range of interest on the whole spectrum. Frequency range, time averaging, auto/manual scales and other facilities may be used to manipulate the recorded signal.

2.3.3 Measurements of Envelope Analysis (Bearcon).

Envelope analysis or bearing condition (bearcon) according to the definition of B&K™ is the technique of amplitude demodulation from amplitude modulated signal. In an attempt to extract more information and find out easier correction between the recorded signals and the faults of gears, envelope analysis spectra are measured for all tested cases.

The result is the time history of the modulating signal. That signal may be studied or interpreted as it is in the time domain, or it may be subjected to a subsequent frequency analysis. Envelope Analysis is the FFT frequency spectrum of the modulating signal. Envelope Analysis can be used for diagnostics investigation of machinery, where faults have an amplitude modulating effect on the characteristic frequencies of the machinery. Envelope analysis (bearcon signature) is very sensitive parameter to analyze the impact effect, and is also an excellent tool for diagnostics of cracks and spallings in Rolling Element Bearings [1].

3. NUMERICAL ANALYSIS

FEA technique was carried out using stress analysis on gear teeth to determine the suitable value of the resistance torque which applied to output gear during tests and to minimize tooth deflection during running, to avoid the interference effect of gear resonance frequencies away from their dynamic performance,

3.1 Static Stress Analysis on Gear Teeth.

In order to carry out the theoretical analysis, a set of 3D identical gears was modeled using CAD software generated using the computer to complete the analysis. Two pair of gears (spur and helical) were created with the exact center distance, face width and material. These gears were virtually checked by using the simulation and animation module of the CAD program. The generated gears were then transferred to the finite element analysis program (ANSYS), to determine von Mises and the principal stresses of gear teeth to ensure a minimum effect of stress on the dynamic performance of gears. Both spur and helical gears were theoretically investigated to determine the suitable braking torque which will apply during the experimental tests to avoid gear failure and excessive tooth deflection. The tooth shape and gear hub were divided into several elements and mesh shape, which depended mainly on the complexity of shape and zone of interests. As shown in Fig. 4, a 3D solid element (solid 73) are used in this analysis, and the average element size is selected to be 0.1 mm with grading factor 1.5 and maximum turn angle 60 deg.

3.2 Modal Analysis and Mode Shapes of the Tested Gears.

A modal analysis technique was carried out on both types of gears by using ANSYS. Moreover, the gear materials and braking load were assigned to finite element analysis.

To ensure the exact interpretation of the recorded frequency spectrum, the resonance frequencies of the gears are extracted from modal analysis. The modal analysis has been carried out three times on each type of gear. The first was when the gears were meshed together; the second was on the large gear alone; and the third last analysis is carried out for was on small gear (pinion) separately. The natural frequency and mode shape were obtained for the first ten modes.

4. RESULTS AND DISCUSSIONS

4.1 Theoretical Analysis

From the FEA program, the stress analysis results showed that the suitable value of the braking torque was found to be 3 N.m which is safe for both types of gears. Additional results showed that the calculated natural frequencies for the meshed gears are slightly

different when compared with the calculated values of the disengaged gears. Table 2 shows a summary of the calculated natural frequencies of spur and helical gears. The mode shapes of the gear teeth at different frequencies were also investigated. The results showed that the gear frequency at the first mode for spur or for helical gears is higher than the range of interest of the measured frequency spectrum, which ranges from 1Hz to 1024 Hz. Consequently, this frequency spectrum range is far from the excitation resonances of the gear box running frequencies, in addition to the gear meshing frequency and its expected side bands.

4.2 The Effect of Teeth Errors on the Time Signal and Vibration Severity.

Complete vibration spectra in time domain and overall vibration severity were recorded. Fig. 5 shows the recorded time spectra for different cases of spur gears. In the case of correct gears, the maximum amplitude of the measured time signals ranges between $\pm$ 2m/sec^2 with frequency equal to the gear meshing frequency (750 Hz). Due to the shaft imperfection, the time signal had been modulated with a relatively low frequency which represents the shaft rotating speed. While, in the case of one gear with tooth error, the time signal includes periodic pulses within the time interval equal to the inverse of the shaft rotating frequency (speed) ($T=1/F_r$). Particularly, for faulty pinion, the pulses occur three times per 0.1. On the other hand, during running of faulty large gear, the results show that one pulse occurs per 0.1 second, or frequency equal to 10Hz. In all cases, all pulses were superimposed (modulated) with high frequency signal that represents the gear mesh frequency. If the two gears were faulty, three pairs of successive pulses were noticed within time interval equal to 0.1 second. New bands appeared near to the gear mesh frequencies, which are called side bands. Moreover, the amplitude of the time signal increases with the present of faulted teeth, and appears as successive pulses that affect time signal. Similarly, Fig. 6 shows the recorded signal during running the faulty helical gear; the same trends and forms were found as the faulty spur gears with some variations in the vibration amplitude. The recorded vibration levels during running helical gear was slightly lower than the values which are measured during running spur gears. For the sake of comparison, Fig.7 shows that, higher overall vibration severity is obtained in the case of two faulty gears with respect to the corrected pair. Referring to the ISO 2372 (10816 table-1) vibration severity of machines operating in the frequency range of 10 to 200 Hz. The vibration values recorded in terms of vibration velocity (mm/sec) were compared with those of the aforementioned standard, the following results were obtained. In the case of correct gears, the gearbox was in good condition range, while, during running with faulty gears, the vibration level increased and became in an unsatisfactory range.

4.3 The Effect of Changing Center Distance on the Time Signal and Vibration Severity.

The center distance between gears were changed by rotating the eccentric bearing housing. The correct pair of helical gear was chosen to study the effect of changing the center distance between gears. Based on the gears configuration, the exact center distance between both spur and helical gears was adjusted to be equal to 101.543 mm. All changes referred to that value, whether negative value (interference) or positive value (clearance or backlash). The results presented in Fig. 8 show the recorded time signals during several changes in center distance of the correct helical gears. The changes start from interference

value equal to (-0.308mm) and end with excessive clearance of (+0.904mm). All collected time signals seem to be the same, with a slight variation, especially in the case of excessive clearance in which the pulses are increased. Fig. 9 shows the overall vibration severity for the different cases of changing center distance. The overall vibration levels in the case of interference are small relative to the exact center distance, due to the increase of mutual interfacial damping of the meshed teeth. It was noticed during tests that long time running in this case will lead to rapid wear as well as teeth failure. Moreover, in case of excessive clearance, the amplitude will increase with the increase of noise level which is noticed during tests. Referring to the ISO 2372, the recorded vibration levels of the gearbox for all cases of interference and correct gears were found in good condition range while the other cases were in an unsatisfactory condition.

4.4 The Effect of Teeth Faults on the Recorded Frequency Response Spectra.

Figs. 10 and 11 show the effect of tooth fault on the measured frequency spectra for different cases of meshed gears. It is clear from the results that these effects are concentrated at the shaft speeds and their higher harmonics as well as the zone of gear meshing frequency and its surrounded side bands. In case pinion contains tooth error, a group of spikes that represents the side bands surrounding the peak signal at the mesh frequency (750Hz) have appeared. It is also noticed from the results that the side bands are located at distances apart from one another by a value equal to the shaft rotating speed, which carries the faulty gear. The distance which measured on the frequency spectra between spikes at the range of gear meshing frequency is equal to 30 Hz in the case of faulty pinion, while it is equal to 10 Hz in the case of faulty large gear. Moreover, the amplitude of the side bands may be larger than the original value of the gear mesh frequency itself, especially in the cases of faulty pinion and both gears are faulty. On the other hand, Fig. 12 shows the effect of error in center distance on the measured frequency spectra. Excessive interference will increase the mutual interfacial damping between meshing teeth and lead to reducing the vibration level. On the other hand, excessive clearance will lead to higher amplitude accompany with noticeable noise level. But with large clearance, the vibration will reduce again due to the decrease of contact area between teeth, which leads to high stresses and rapid failure.

4.5 Envelope analysis (Bearcon)

The demodulation process in the envelope analysis technique will damp the range of gear meshing frequency and its surrounding side bands. However, the amplitude of the shaft speed and its higher harmonic are improved and become higher and clearer. Figs. 13 and 14, show the case of correct gears. The dominant peaks are located only at the shafts speed (10Hz and 30Hz) with some peaks at the higher harmonics of the input shaft due to shaft imperfection. However, in the case of pinion with tooth error, the peaks are located at the speed of input shaft and its higher harmonics. But if the two gears contain teeth error, high peaks appear along the envelope spectrum, spaced by 10 Hz. The peaks at the pinion speed and its harmonics are still higher because the fault on the pinion is much deeper as compared with the fault on the large gear which leads to deep impacts. The same trend is given for two faulty gears. Fig. 15 shows the effect of changing the center distance on the envelope analysis. That effect is concentrated at the input and output

shaft speeds rather than their higher harmonics. In these cases, the damage index is the main parameter which is used to measure the vibration signal.

5. CONCLUSIONS AND RECOMMENDATIONS.

This work addressed the effect of manufacturing errors on the dynamic performance of gears. Experiments were carried out to present the correlation between the main gear manufacturing error and the measured dynamic response signals. Damages in gear teeth and error in center distance between gears were tackled for both straight spur and helical gears. The following conclusions can be confirmed:

1- In most cases, the resonance frequencies of the gears did not affect their dynamic performance, especially in the range of normal working speeds.
2- Analysis of overall vibration severity is only useful for judging the overall condition of gearbox.
3- Time response signal may be useful to predict fault diagnosis of gears, rather than the error in the center distance between gears.
4- Frequency response signals are still among the best methods used for investigating the fault diagnosis of gearbox.
5- Envelope spectrum is useful as a comparative method, and may be used in vibration monitoring technique.
6- Interference in the center distance of gears may appear as a misleading effect on the dynamic performance of gears, due to the increase of interfacial damping.
7- Clearance (backlash) between meshed gears is useful to some extent after which bad effect will appear.

Suggestions for further work:

This work focused on gear faults which contain one-tooth errors. Future work can be extended to:

1- Cepstrum analysis and other advanced techniques, which may give more detailed information for fault diagnosis.
2- It is preferred to the study of the misalignment of shafts which carry the gears, in addition to changing center distance.
3- The investigation of gear faults which contain more than one tooth error, or random teeth errors.
4- Experiments may be extended to other types of gears, such as helical gears bevel gears and worm wheel.

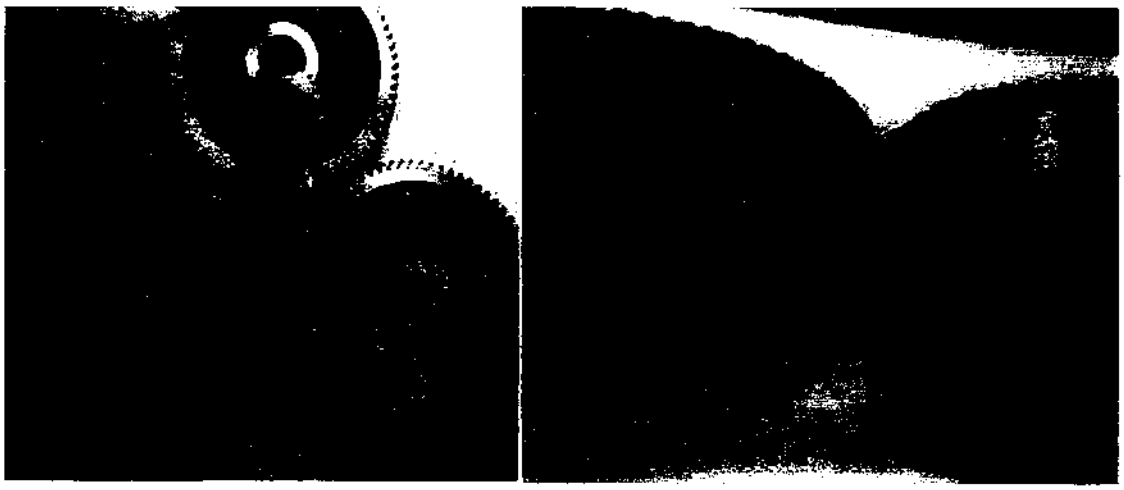

Fig.1 Set of three pair gears (the three mounted in the gearbox).

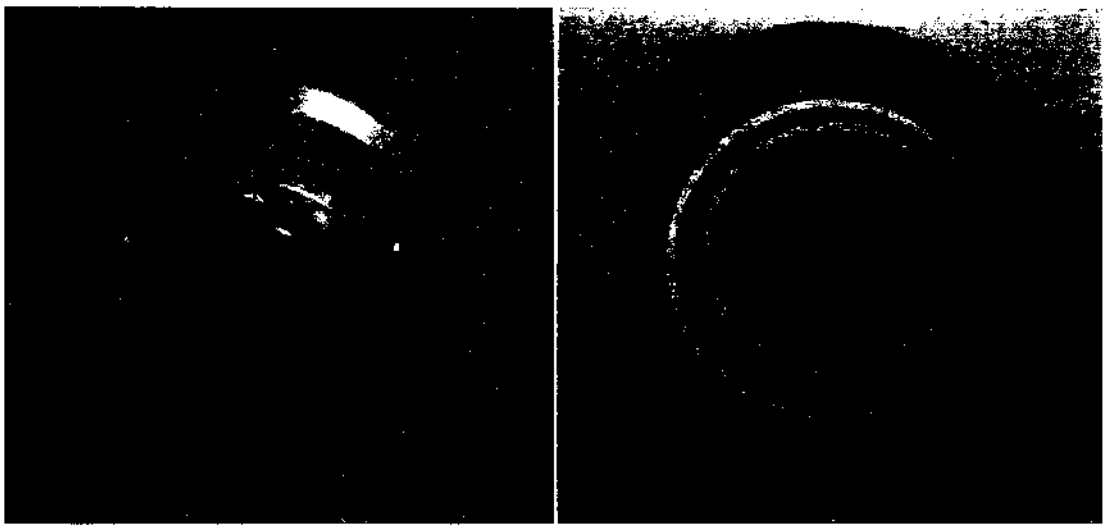

Fig. 2 Eccentric bearing housing designed to provide several changes in the center distance between gears

1-Drive unit 2- Coupling 3- Speed Sensor 4- Gear Box

5- Speed Controller 6- Coupling 7- Breaking unit 8- Breaking Controller

Fig.3 Test rig prepared for gear testing

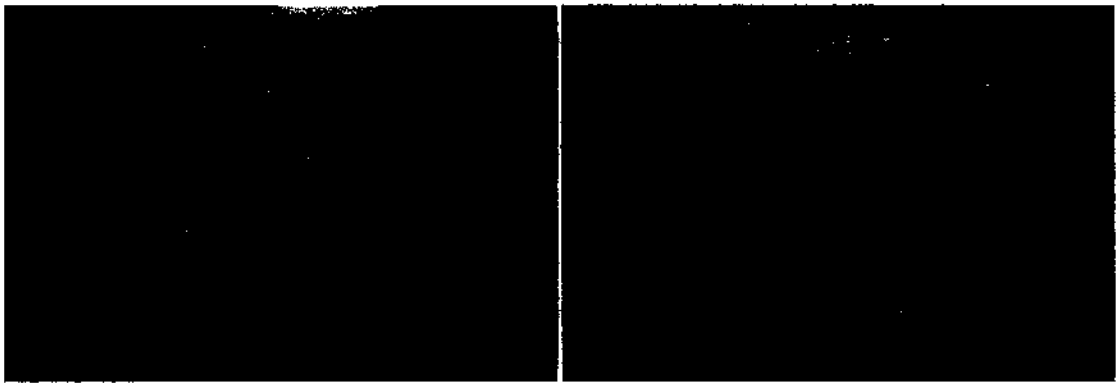

Fig. 4 FEA theoretical calculation of stress and modal analysis of spur and helical gears.

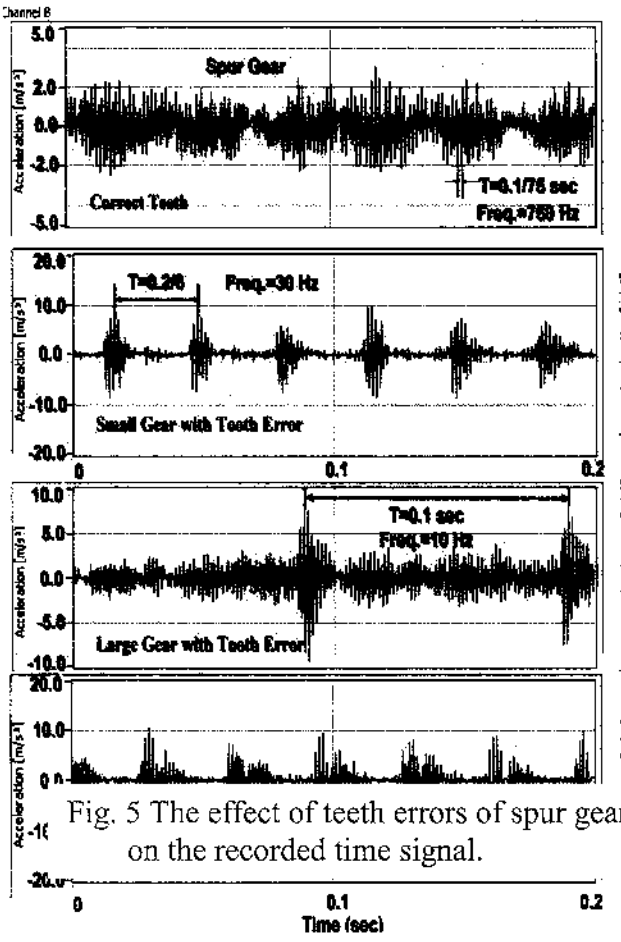

Fig. 5 The effect of teeth errors of spur gear on the recorded time signal.

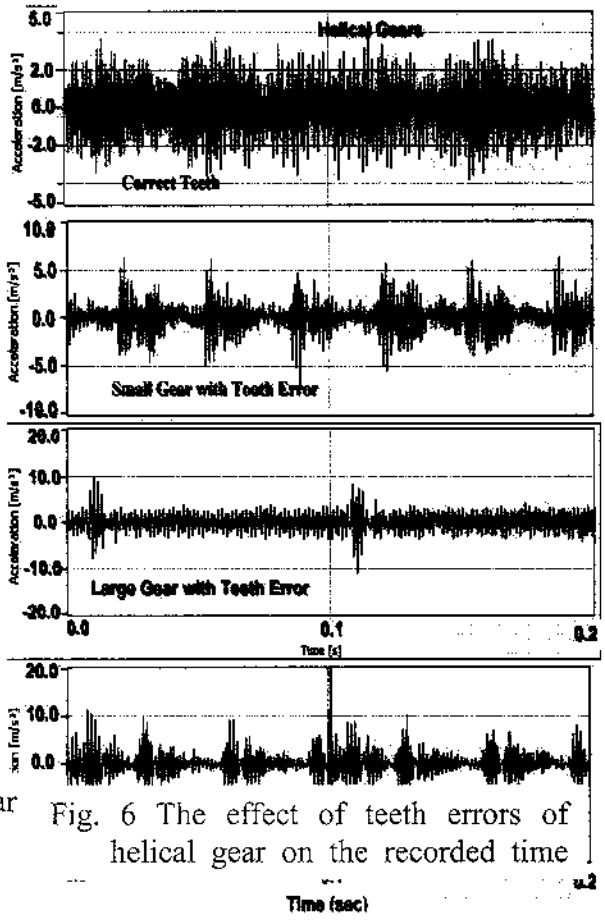

Fig. 6 The effect of teeth errors of helical gear on the recorded time

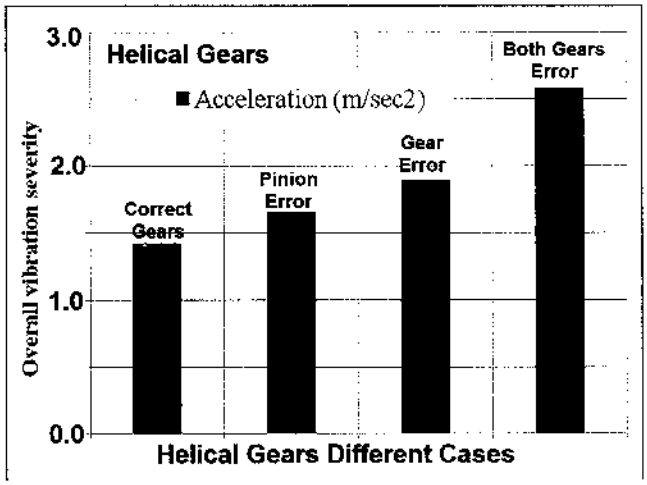

Fig. 7 The effect of teeth errors of helical gear on the overall vibration severity.

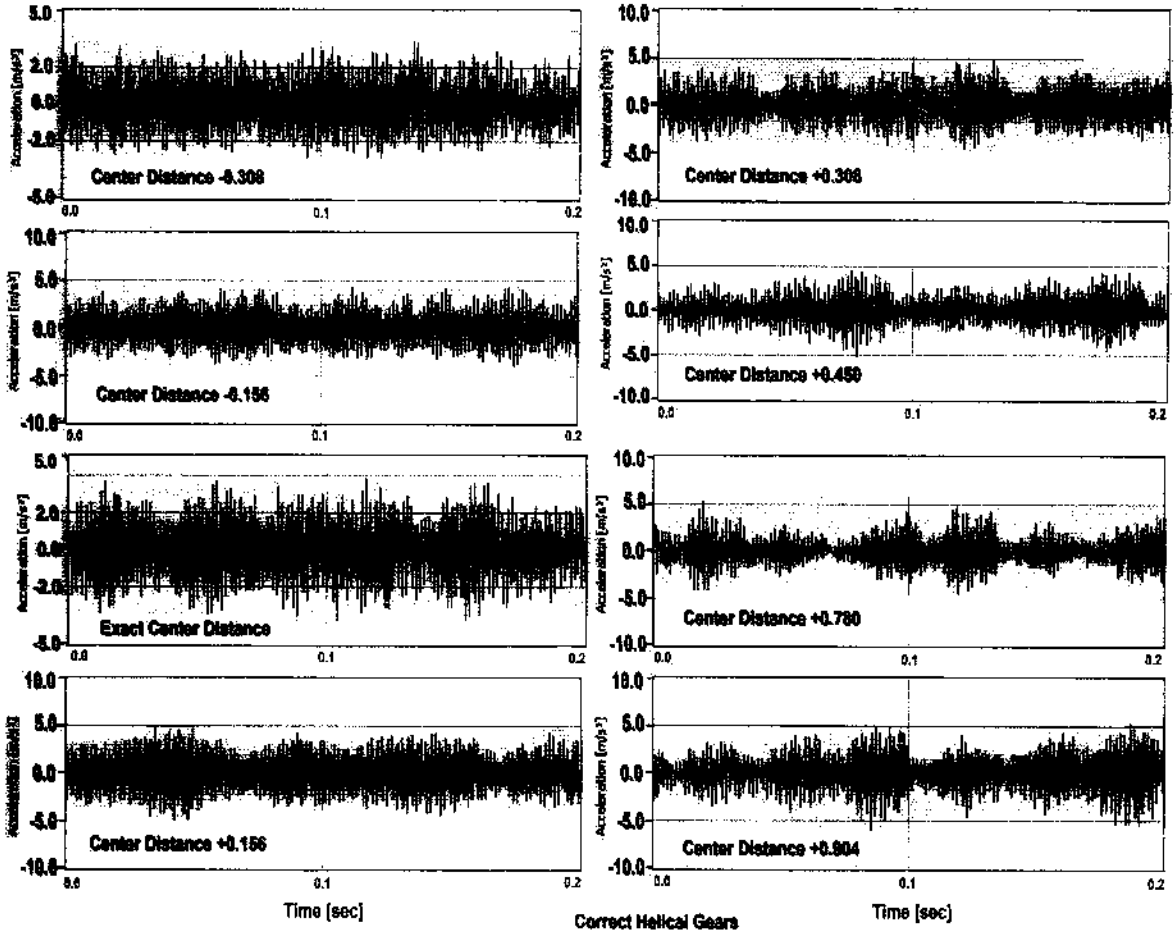

Fig.8 The effect of changing the center distance of correct helical gears on the recorded time signals.

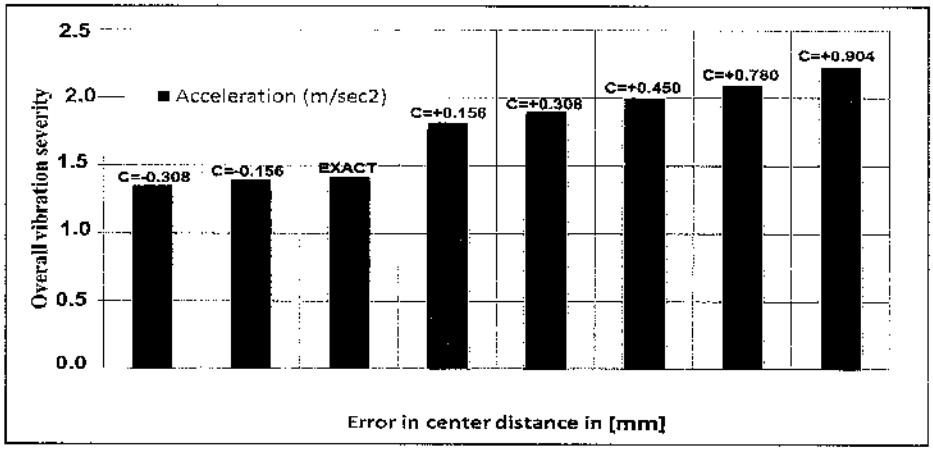

Fig.9 The effect of changing the center distance of helical gear on the overall vibration severity.

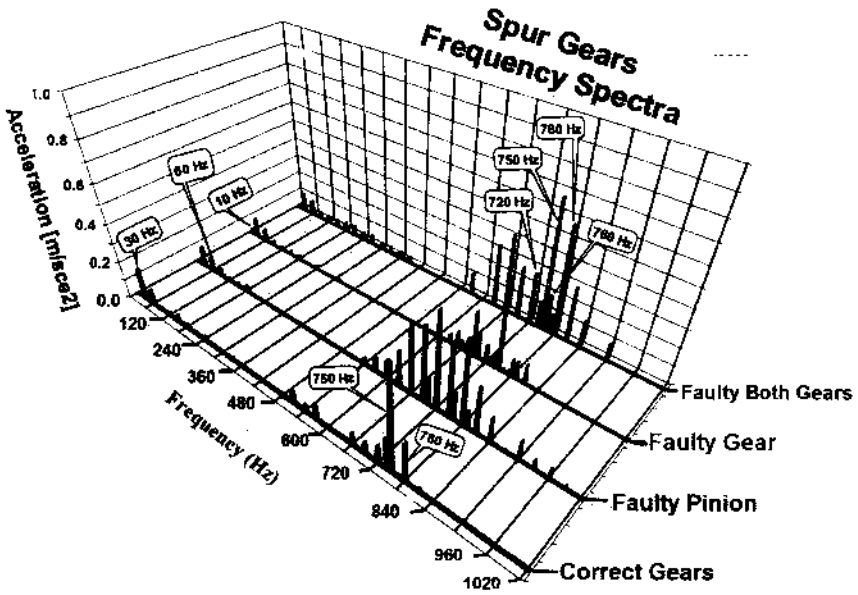

Fig.10 The effect of teeth errors of spur gear on the recorded frequency spectra

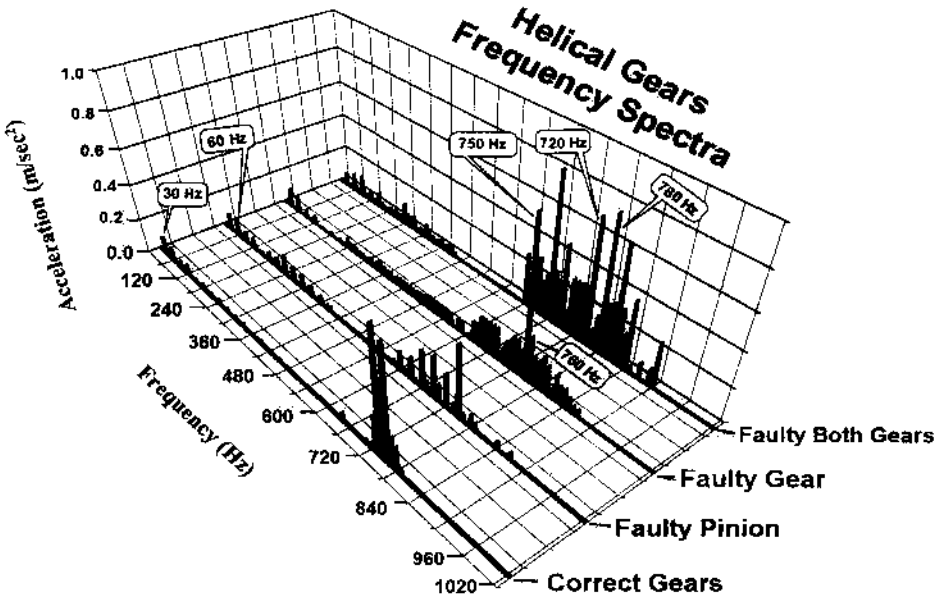

Fig. 11 The effect of teeth errors of helical gear on the recorded frequency spectra

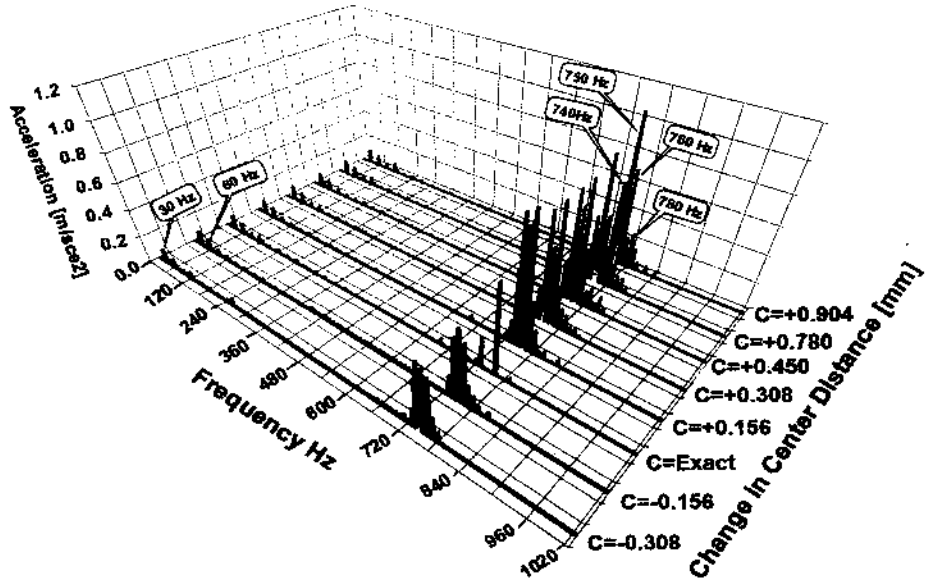

Fig. 12 The effect of changing the center distance of correct helical gear on the recorded frequency spectra

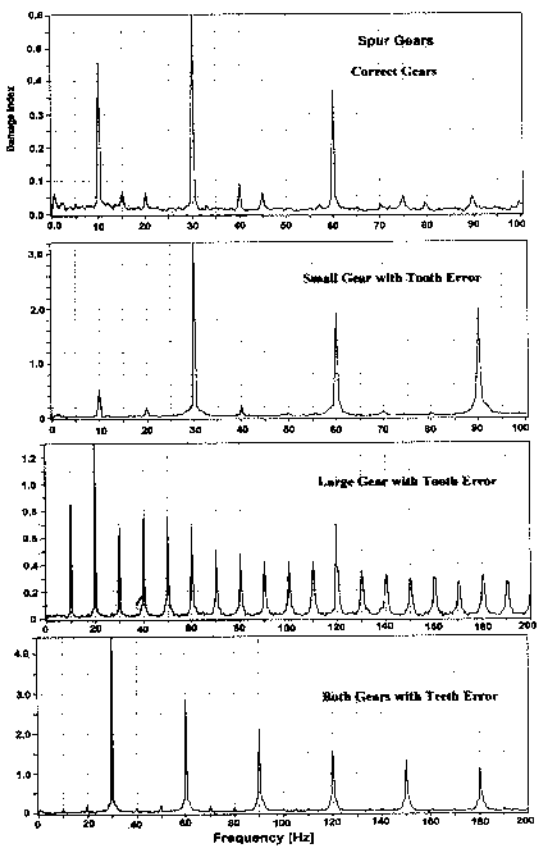

Fig. 13 Envelope analysis for different cases of spur gears

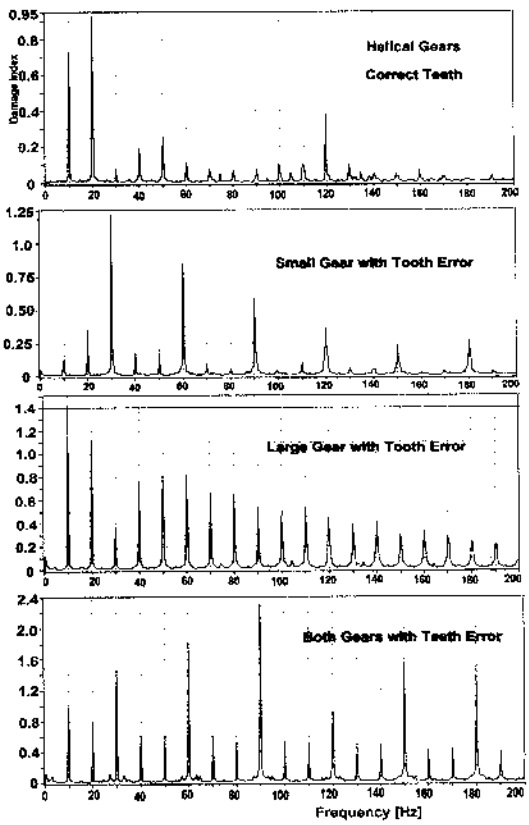

Fig. 14 Envelope analysis for different cases of helical gears

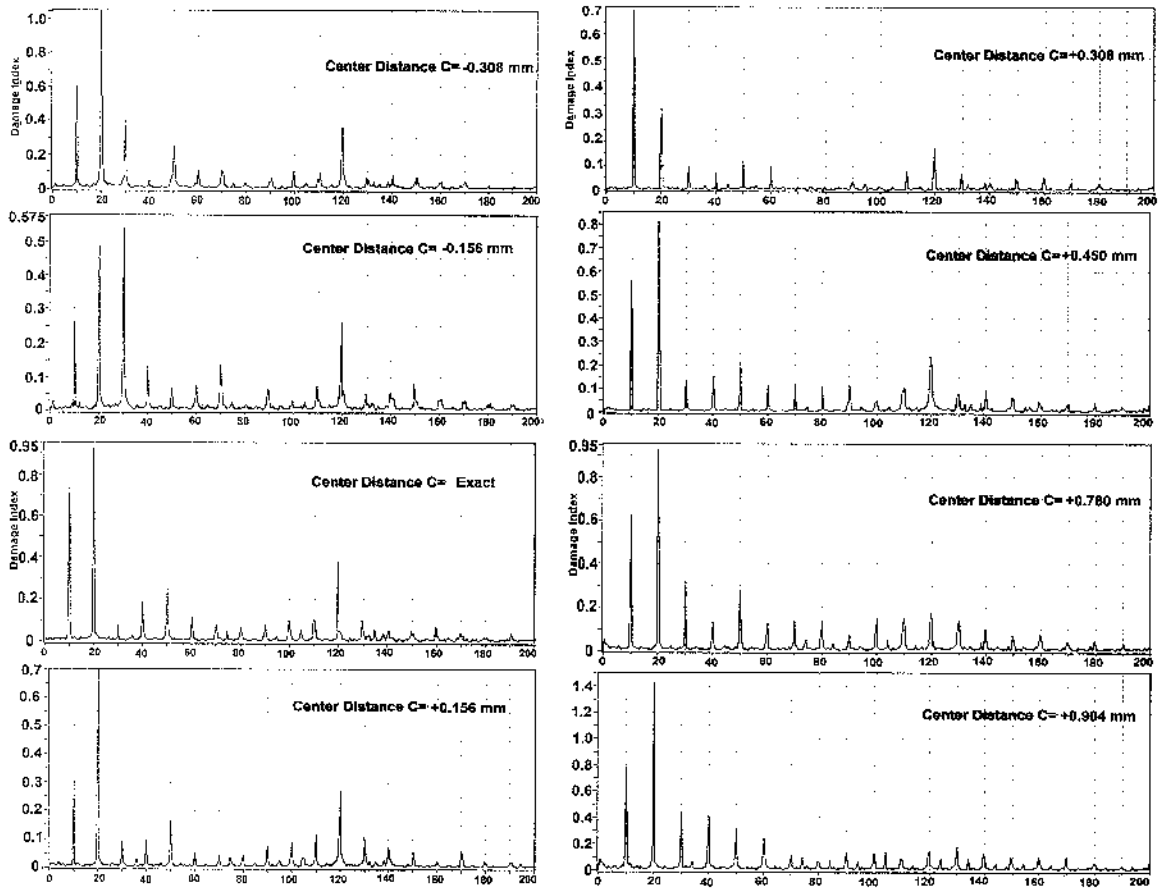

Fig. 15 Envelope analysis for different changes in center distance of helical gears

Table 1. Relation between the angular position of bearing housing and error in center distance

Housing Position (deg °)	Centre distance (mm)	Error in center distance (mm)
-20	101.232	-0.308
-10	101.384	-0.156
0	101.54	0
10	101.696	0.156
20	101.848	0.308
30	101.99	0.45
60	102.32	0.78
90	102.444	0.904

Table 2. The FE results of the natural frequencies of gears

	Mode Frq.	Meshed Gears	Disengaged Large Gear	Disengaged Small Gear
Spur Gears	F1(Hz)	1921.13	1866.52	55092.60
	F2(Hz)	2021.38	1866.96	58770.15
	F3(Hz)	2322.93	2118.94	58828.70
	F9(Hz)	9586.78	9353.41	65783.91
	F10(Hz)	9894.61	9374.83	65805.14
Helical Gears	F1(Hz)	1956.80	1893.73	53264.70
	F2(Hz)	2049.16	1896.09	56674.51
	F3(Hz)	2348.49	2146.15	56850.04
	F9(Hz)	9691.36	9376.93	64170.51
	F10(Hz)	10032.05	9379.59	64186.66

REFERENCES

1- Hans Konstantin-Hansen, Brüel&Kjær, "Envelope Analysis for Diagnostics of Local Faults in Rolling Element Bearings" Denmark BO 0501–11 02/03 Rosendahls Bogtrykkeri.

2- Jafarizadeh, R. Hassannejadb, M.M. Ettefaghb, S. Chitsaz." Asynchronous input gear damage diagnosis using time averaging and wavelet filtering", Mechanical Systems and Signal Processing 22 (2008) 172–201.

3- Yu Yang a, Yigang He, Junsheng Cheng a, Dejie Yu. "A gear fault diagnosis using Hilbert spectrum based on MODWPT and a comparison with EMD approach", *Measurement*.2008.09.011, 2008 Elsevier Ltd.

4- Lei, Y., Zuo, M.J., He, Z., Zi, Y., "A multidimensional hybrid intelligent method for gear fault diagnosis", *Expert Systems with Applications* (2009), doi: 10.1016 / j.eswa.2009.06.060

5- Parey A., et al, "Dynamic modeling of spur gear pair and application of empirical mode decomposition-based on statistical analysis for early detection of localized tooth defect", *Journal of Sound and Vibration* 294 (2006) 547–561.

6- D. Wanga, Q. Miaoa, RuiKang, "Robust health evaluation of gearbox subject to tooth failure with wavelet decomposition", *Journal of Sound and Vibration* 324 (2009) 1141–1157.

7- T.H. Loutas, G. Sotiriades, I. Kalaitzoglou, V. Kostopoulos, "Condition monitoring of a single-stage gearbox with artificially induced gear cracks utilizing on-line vibration and acoustic emission measurements", *Applied Acoustics* 70 (2009) 1148–1159.

8- N. Saravanan, K.I. Ramachandran, "Fault diagnosis of spur bevel gear box using discrete wavelet features and Decision Tree classification", *Expert Systems with Applications* 36 (2009) 9564–9573.

9- N Jian-Da Wu, Chuang-Chin Hsu, "Fault gear identification using vibration signal with discrete wavelet transform technique and fuzzy–logic inference", *Expert Systems with Applications* 36 (2009) 3785–3794.

10- X. Fan, M. J. Zuo, "Gearbox fault detection using Hilbert and wavelet packet transform", *Mechanical Systems and Signal Processing* 20 (2006) 966–982.

11- N. Saravanan, S. Cholairajan, K.I. Ramachandran, "Vibration-based fault diagnosis of spur bevel gear box using fuzzy technique", Expert Systems with Applications 36 (2009) 3119–3135.

12- S.J. Loutridis, "Gear failure prediction using multiscale local statistics", *Engineering Structures* 30 (2008) 1214–1223.

13- W.Bartelmus, R.Zimroz, "A new feature for monitoring the condition of gearboxes in non- stationary operating conditions", *Mechanical Systems and Signal Processing* 23 (2009) 1528–1534.

14- M. Inalpolat, A. Kahraman, "A theoretical and experimental investigation of modulation sidebands of planetary gear sets", *Journal of Sound and Vibration* 323 (2009) 677–696

15- Wilson Wang, DerekKanneg, "An integrated classifier for gear system monitoring", *Mechanical Systems and Signal Processing* 23 (2009) 1298–1312.

16- W.D. Marka,C.P. Reagor, D.R. McPherson, "Assessing the role of plastic deformation in gear-health monitoring by precision measurement of failed gears", *Mechanical Systems and Signal Processing* 21 (2007) 177–192.

17- Chaari F.,et al "Effect of spalling or tooth breakage on gearmesh stiffness and dynamic response of a one-stage spur gear transmission", *European Journal of Mechanics* A/Solids 27 (2008) 691–705.

18- Siyan Wu, Ming J. Zuo_, Anand Parey," Simulation of spur gear dynamics and estimation of fault growth", *Journal of Sound and Vibration* 317 (2008) 08–624.

19- N. Sawalhi , and R.B. Randall, "Simulating gear and bearing interactions in the presence of faults Part II: Simulation of the vibrations produced by extended bearing faults", *Mechanical Systems and Signal Processing* 22 (2008) 1952–1966.

20- N. Sawalhi, and R.B. Randall, "Simulating gear and bearing interactions in the presence of faults Part I. The combined gear bearing dynamic model and the simulation of localised bearing faults", Mechanical Systems and Signal Processing 22 (2008) 1924–1951.

21- M. Amarnath, C.Sujatha, S.Swarnamani, "Experimental studies on the effects of reduction in gear tooth stiffness and lubricant film thickness in a spur geared system", *Tribology International* 42 (2009) 340–352.

22- J. Hongkai, H. Zhengjia, D. Chendong, Chen Peng, "Gearbox fault diagnosis using adaptive redundant Lifting Scheme", *Mechanical Systems and Signal Processing* 20 (2006) 1992–2006.

23- Jean Luc Dion, et al, "Gear impacts and idle gear noise: Experimental study and non-linear dynamic model", *Mechanical Systems and Signal Processing* (2009), doi:10.1016/j. ymssp.2009.05.007.

Received 2/4/1432;7/3/2011, accepted 25 /4 /1433; 18/3/2012

المجلد ٤ العدد ٢ - رجب ١٤٣٣هـ يونية ٢٠١٢م

الجزء الأول: البحوث العلمية باللغة العربية.

لا توجد بحوث باللغة العربية مقدمة في هذا العدد.

الجزء الثاني: البحوث العلمية باللغة الإنجليزية.

ميكانيكا

المجلة تفتح صفحاتها للإعلانات

للإعلان في المجلة يمكن الاتصال بمجلة جامعة أم القرى للهندسة والعمارة ، ص. ب. ٧١٥

جامعة أم القرى ، مكة المكرمة ، المملكة العربية السعودية

بريد إلكتروني jea@uqu.edu.sa

http://www.uqu.edu.sa

1433/247/1433-2012 © The University Press

تعهد نشر بحث

اسم الباحث / الباحثة : ----------

المرتبة العلمية: ----------

القسم العلمي: ----------

الكلية: ----------

الجامعة: ----------

عنوان البحث: ----------

الباحثين المشاركين (إن وجد): ----------

أتعهد أنا الموقع اسمي أدناه بأن البحث لم يسبق له النشر أو مقدم للنشر في مجلة علمية أخرى محلياً أو دولياً، وأن التزم بقواعد النشر بمجلة جامعة أم القرى للهندسة والعمارة. والله ولي التوفيق ...

الباحث التاريخ: / / ١٤هـ

رقم الإيداع ٢٤٧/١٤٣٣

1433/247/1433-2012 © The University Press

إرشادات المؤلفين

تستقبل هيئة تحرير مجلة جامعة أم القرى للهندسة والعمارة الأبحاث الأصلية والمراجعات العلمية والتقارير العلمية التي لم يسبق نشرها جزئياً أو كلياً ولم تقدم للنشر لجهة أخرى. تخضع الأعمال المقدمة لمراجعة هيئة التحرير وتحكيم متخصصين. تعتمد سياسة النشر على أصالة البحث وقيمته العلمية. يقدم العمل مطبوع على ورق أبيض مقاس A4، أصل وأربع صور. تكون الطباعة على وجه واحد مع ترك فراغ مزدوج بين السطور والهوامش لا يقل عن ٣سم في كل اتجاه، يستخدم الخط Simplified Arabic Fixed بحجم ١٤عادي في كتابة متن البحث وحجم ١٤ أسود للعناوين الرئيسة. يرسل العمل لرئيس التحرير مع رسالة لطلب النشر وفي حالة أكثر من مؤلف يرفق تفويض للباحث المسئول مع أسماء الباحثين المشاركين، والإشارة إلى مجال تخصص البحث المرسل "العام والدقيق".

تسلسل المحتوى يكون كالتالي:

- صفحة عنوان البحث مع أسماء المؤلفين والجهات العلمية التي ينتمون إليها مع ذكر اسم وعنوان الباحث.
- صفحة عنوان البحث فقط.
- صفحة الخلاصة تتبعها كلمات للفهرس.
- المحتوى يكون حسب التسلسل التالي: المقدمة، الطرق المعملية والمواد والعينات، النتائج، المناقشة، المراجع، الشكر والتقدير، الجداول، الرسومات البيانية، الصور الفوتوغرافية، تذيل الجداول والرسومات البيانية والصور الفوتوغرافية. يبدأ الترقيم من صفحة عنوان البحث.

عنوان البحث: يجب أن لا يتجاوز عنوان البحث عشرين كلمة وأن يتناسب مع مضمون البحث ويدل عليه أو يتضمن الاستنتاج الرئيسي (حجم الخط ١٨ أسود).

المؤلفون: يكتب على النحو التالي:

في حالة اللغة العربية: الاسم الأول _____ الأب _____ اللقب _____.

في حالة اللغة الإنجليزية: الاسم الأول _____ الحرف الأول من اسم الأب _____ اللقب.

ويكتب مع كل اسم المؤسسة العلمية التي يتبعها، ويحدد الباحث المسؤول، ويعطي عنوان المراسلة بالكامل بما في ذلك أرقام التليفون – الفاكس – والبريد الإلكتروني. لا داعي لذكر المؤهلات العلمية ويكتفي بذكر الدرجة العلمية (حجم الخط ١٤ أسود).

الخلاصة: تكتب الخلاصة باللغة العربية وأخرى باللغة الإنجليزية في حدود ٢٥٠–٣٠٠كلمة وان تحتوي على الهدف وما تم عمله وما تحقق والاستنتاج وأن تعطي بمفردها فكرة واضحة عن البحث وإن ذكرت أرقام يجب أن تكون مطابقة لما ورد ذكره في محتوى البحث مع نتيجة المعالجة الإحصائية ولا تذكر مراجع (رجاء ذكر عدد الكلمات في نهاية الخلاصة بين قوسين).

رقم الإيداع ٢٤٧/١٤٣٣

1433/247/1433-2012 © The University Press

هدف و مجال المجلة

المجلة دورية علمية محكمة تصدر عن جامعة أم القرى بواقع عددين في السنة. وتهدف المجلة إلى نشر الأبحاث الأصيلة والمراجعات العلمية للأبحاث والتقارير العلمية باللغة العربية أو الإنجليزية التي لم يسبق نشرها أو تقديمها للنشر لدي جهات أخرى – بعد مراجعتها من قبل هيئة التحرير وتحكيمها من قبل المختصين .

ترسل جميع الأعمال والاستفسارات مباشرة إلى رئيس التحرير

جميع البحوث المقبولة تئول ملكيتها للمجلة

رقم الإيداع ٢٤٧/١٤٣٣

1433/247/1433-2012 © The University Press

الصورة الفوتوغرافية: مقاس الصورة لا تتجاوز أبعادها ١٢سم عرضاً × ١٠سم طولاً، وأن تكون مطبوعة على ورق لامع صقيل واضحة تمكننا من طباعتها أو مطبوع بواسطة طابعة ليزر إذا كانت مأخوذة بكاميرا رقمية. ترسل خمس أصول لكل صورة يكتب عنوان الصورة في أسفل الصورة بحيث يدل بدقة على محتوى الصورة وما تدل عليها دون الحاجة للرجوع إلى متن البحث. ويكتب خلق الصورة بالقلم الرصاص صورة رقم (x) مع ذكر اسم المؤلف المسؤول.

التعديلات والمراجعة النهائية: تتم التعديلات المقترحة من قبل المحكمين وفقاً لما أُقترح وتكون المراجعة النهائية مسؤولية المؤلف دون إجراء أي تعديلات جديدة، وترسل إلى رئيس التحرير في خلال ثمانية أسابيع من تاريخ إرسالها إلى المؤلف وإلا يخضع العمل لإعادة التحكيم. ويرفق معه البحث على سي دي مع صورة مطبوعة على ورق مقاس A4 (الجهاز المستخدم IBM أو أي جهاز متوافق معه).

المستلات: ترسل للمؤلف خمسة عشر مستلة من البحث مجاناً وبإمكانه طلب المزيد أثناء إرسال البروفات (تحدد التسعيرة على استمارة الطلب).

نقل حقوق الطبع: عند قبول البحث للنشر يتم تحويل ملكية النشر من المؤلف إلى المجلة.

الرموز: يجب استخدم الرموز والمختصرات والمصطلحات المعتمدة (SI Units).

المراسلات: جميع الأعمال والاستفسارات ترسل مباشرة إلى رئيس تحرير مجلة جامعة أم القرى للهندسة والعمارة. مجلة الجامعة، ص.ب. ٧١٥، جامعة أم القرى، مكة المكرمة،
البريد الإلكتروني: **jea@uqu.edu.sa**

التبادل والإهداء: توجه الطلبات إلى عمادة شئون المكتبات، جامعة أم القرى.

سعر الاشتراك السنوي: (مائة ريالاً) أو (أربعون دولاراً) بما في ذلك أجور البريد.

1433/247/1433-2012 © The University Press

الكلمات التي تستخدم للفهرسة: لا تتجاوز عشرة كلمات. ويتم اختيارها بما يتواكب مع المصطلحات التي تصدر من قبل هيئات رصد الأبحاث.

المقدمة: تتضمن المقدمة بوضوح دواعي إجراء البحث (الهدف) وتساؤلات وفرضيات البحث مع ذكر الدراسات السابقة ذات العلاقة بحيث لا يتجاوز إجمالي عدد المراجع المستخدمة في المقدمة ١٥مرجعاً. وعدم عرض أي من النتائج أو المناقشة أو الاستنتاج في المقدمة.

الطرق البحثية والمعملية والأدوات المستخدمة: يجب أن تكون واضحة وصالحة وملائمة لتحقيق الهدف، وتتوفر فيها الدقة العلمية.

النتائج: تجنب التكرار في عرض النتائج والسرد الحرفي لأرقام الجداول والرسومات البيانية. وأن يكون العرض واضحاً ومترابطاً مدعماً ومعالجاً إحصائياً مع بيان ارتباطها بهدف وتساؤلات البحث. عدم تكرار المعلومات في الجداول والرسومات البيانية.

المناقشة: تحليل النتائج تحليلاً موضوعياً هادفاً في ضوء المعلومات المتوفرة (بعيداً عن تكرار سرد النتائج) مع ربطها بالدراسات السابقة وأن تشمل الاستنتاج المنبثق والمدعم عن النتائج المتوفرة في الدراسة.

الشكر والتقدير: يستحسن ذكر الجهة المدعمة للبحث والأشخاص أو الجهات التي يريد الباحثون شكرهم لمساهمتهم بصورة أو أخرى في البحث.

المراجع: تذكر في المتن حسب تسلسل ورودها (الاسم والسنة)، وضرورة التقيد بدقة التوثيق وأن تكون ذات علاقة فعلية بموضوع البحث، وتسرد كافة المراجع في قائمة المراجع بنهاية البحث بصورة أبجدية. يتم البدء بلقب المؤلف ثم اسمه ثم العنوان ثم المجلد ثم سنة النشر (انظر إرشادات المؤلفين باللغة الإنجليزية).

الجداول: الجدول يكتب على صفحة منفردة ومقاس الجدول لا يتجاوز ١٣×١٨سم وأن تكون الأرقام والمعلومات المدونة في الجداول واضحة ومقروءة دون الحاجة إلى التكبير. في أعلى الجدول يكتب رقم الجدول على النحو التالي جدول رقم(١) وعنوان يدل بدقة على محتوى المعلومات دون الرجوع إلى رقم الجدول وعنوانه (يرسل الأصل مع أربع نسخ أخرى).

الرسومات البيانية: كل رسم بياني يكتب على صفحة منفردة، مقاس الرسم البياني لا يتجاوز: ١٢سم عرضاً × ١٠سم طولاً وأن تكون اللوحة البيانية واضحة ومقروءة بحيث يمكن تصويرها مباشرة دون الحاجة إلى التكبير أو التصغير. (أن تكون الرسوم البيانية مصورة فوتوغرافيا على ورق صقيل أو بواسطة طابعة ليزر في حالة إنتاجها بواسطة الحاسب الآلي). ترسل خمسة أصول لكل رسم ولا تقبل الصور. يكتب عنوان الرسم البياني في أسفل الرسم بحيث يدلل بدقة على محتوى المعلومات في الرسم البياني دون الحاجة للرجوع إلى متن البحث ويكتب خلف الصفحة بالقلم الرصاص رقم الرسم البياني شكل رقم (x) مع ذكر اسم المؤلف المسؤول.

1433/247/1433-2012 © The University Press

رقم الإيداع ٢٤٧/١٤٣٣


بسم الله الرحمن الرحيم

مجلـــة جامعـة أم القـرى

للهندسة والعمارة

المجلد ٤ العدد ٢ رجب ١٤٣٣ هـ - يونية ٢٠١٢ م

مجلة دورية علمية محكمة تصدر عن جامعة أم القرى
وتهدف لنشر الأبحاث الأصيلة والمراجعات العلمية للأبحاث
والتقارير العلمية باللغة العربية أو الانجليزية التي لم يسبق
نشرها أو تقديمها للنشر لدى جهات أخرى.

رد مد : ١٦٥٨-٤٦٣٥